DISCLAIMER NOTICE

THIS DOCUMENT IS BEST QUALITY PRACTICABLE. THE COPY FURNISHED TO DTIC CONTAINED A SIGNIFICANT NUMBER OF PAGES WHICH DO NOT REPRODUCE LEGIBLY.

AD No. 122229

DATE 6 MAY 1957

Bureau of Ships Technical Library
Code 312, Room 1528 Main Navy Bldg.
Washington 25, D. C.

(a) ASTIA ltr of 2/21/57 to BUSHIPS

RETURN OF LOAN

(Unclassified)

...guide Systems" for April 1956 on Nober-63295

...bers of commercial confidence may be included ...quested that proprietary interests be safe-

...ay to know

Marion E. Bonnicelli

...PLEASE SIGN DUPLICATE

61 25250

HANDBOOK ON BREAKDOWN OF AIR IN WAVEGUIDE SYSTEMS

by Dr. Lawrence Gould

MICROWAVE ASSOCIATES, INC.
22 Cummington Street
Boston 15, Massachusetts

NAVY DEPARTMENT, BUREAU OF SHIPS, ELECTRONICS DIVISION
CONTRACT Nobsr 63295 "MICROWAVE HIGH POWER BREAKDOWN STUDY"
INDEX NO. NE-111616 APRIL 1956

MICROWAVE Associates INCORPORATED

TABLE OF CONTENTS

ABSTRACT

A theory of microwave breakdown in air capable of predicting the electric field strengths at breakdown as a function of geometry, frequency, pressure, and pulse width is used in computing the power handling capacities of conventional waveguide systems. Rectangular, coaxial, and cylindrical waveguides are considered for both cw and pulsed breakdown. The TE_{11}, TE_{01}, and TM_{01} modes of operation in cylindrical waveguide are treated. Curves for the breakdown electric field are presented as a function of experimental parameters so that the power handling capacity can be computed for any set of conditions. Typical curves for the breakdown power as a function of pressure and pulse width are presented for the common waveguide systems. The effects of repetition rate, pulse shape, standing waves, gas temperature, and external radiation are discussed.

REFERENCES

1. T. Moreno, "Microwave Transmission Design Data", (McGraw-Hill, 1948).

2. G. L. Ragan, "Microwave Transmission Circuits", Rad. Lab. Series No. 9, (McGraw-Hill, 1948).

3. RMA, "Standard For Rigid Rectangular Waveguides", TR-108 (Feb., 1949).

4. P. H. Smith, "RF Transmission Line Nomographs", Electronics, Vol. 22, No. 2, Pgs. 112-7, (Feb., 1949).

5. H. A. Wheeler, "Breakdown Voltage In Air At High Frequencies", Wheeler Labs. Report 416, (May 2, 1950).

6. Armed Services, "List Of Standard Rigid Rectangular Waveguides", ASESA, (Feb. 12, 1952).

7. H. A. Wheeler, "Pulse-Power Chart For Waveguides And Coaxial Lines", Wheeler Labs., Monograph No. 16, (April, 1953).

8. L. Gould & L. W. Roberts, "The Breakdown Of Air At Microwave Frequencies", Microwave Associates, Inc., MA-1, (Dec., 1955).

9. R. Cooper, J. Of I.E.E., Vol. 96, Part III, p. 315, (1947).

10. "Handbook Of Chemistry And Physics", 34th Edition, (1952-1953).

I. PURPOSE

Numerous articles on the power handling capacity in air of standard waveguide systems have been reported in which the effects of waveguide size, frequency, and gas pressure have been included.[1-7] The calculations of power handling capacity in these reports are based on the assumptions that the maximum electric breakdown field is 30kv/cm at atmospheric pressure and that the breakdown power is proportional to the square of the pressure. Recent work at Microwave Associates, Inc.[8] under Navy contract *Nobsr63295* has proven that the above assumptions are incorrect. A theory for breakdown in air at microwave frequencies was developed and verified over a wide range of experimental parameters. The availability of a working theory of breakdown, capable of predicting the breakdown electric field as a function of pressure, frequency, pulse width, and geometry, necessitates a recalculation of the power handling capacities of the standard waveguide systems. In this handbook the theory is applied to predicting the breakdown power capacities of rectangular, coaxial, and circular waveguides as a function of experimental parameters. The calculations are performed for the most common waveguide sizes and frequencies and are presented in both graphical and tabular form. However, from the curves presented, the power handling capacity can be calculated for any particular waveguide size and frequency. A qualitative description of the phenomena controlling breakdown is discussed so that the application of the theory to practical systems can be better understood and properly utilized.

II. SYMBOLS

- n - electron density (electrons per c.c.)
- ν_i - frequency or number of electrons ionized per second per electron
- ν_a - frequency or number of electrons attached per second per electron
- D - electron diffusion coefficient
- P_o - pressure normalized to 20°C(293°K) (mm Hg)
- p - pressure at any temperature (mm Hg)
- E_{rms} - rms value of the microwave field (volt/cm)
- E_e - effective d.c. field (volt/cm)
- λ - free space wavelength (cm)
- ω - radian frequency of applied field (radians/second)
- ν_c - electron collision frequency $(5.3 \times 10^9 p_o)$ (collisions/sec)
- τ - power pulse width (sec)
- d - separation between two infinite parallel plates
- $\langle \nu_i - \nu_a \rangle / p_o$ - time average of $(\nu_i - \nu_a)/p_o$
- P - microwave power (watts)
- T - gas temperature (°K)
- f_1, f_2 - lower and upper limits of rated frequency range of waveguide
- λ_c - cut-off wavelength (cm)
- λ_g - guide wavelength (cm)
- a,b - width and height of rectangular waveguide (cm)
- r_1, r_2 - radii of inner and outer conductors of coaxial waveguide (cm)
- r_o - radius of cylindrical waveguide (cm)

III. THEORY OF BREAKDOWN

In a high frequency gas discharge breakdown, the primary ionization due to the electron motion is the only production mechanism which controls breakdown. The discharge breakdown occurs when the production in electron density due to the ionization of the gas becomes greater than or equal to the loss of electrons by diffusion to the surrounding walls and attachment to neutral gas molecules. A detailed study of the build-up of the discharge is obtained from considering the continuity equation for electrons

$$\partial n/\partial t = \nu_i n - \nu_a n + \nabla^2(Dn) \qquad (1)$$

Eq. (1) states that the net number of electrons produced per second, $\partial n/\partial t$, is equal to the number of electrons produced per second by ionization, $\nu_i n$, less the number of electrons lost per second by attachment, $\nu_a n$, and the number of electrons lost per second by diffusion, $-\nabla^2(Dn)$. The coefficients ν_i, ν_a, and D are obtained as a function of electron average energy from measurements of drift velocity, average energy, Townsend ionization coefficient, and attachment coefficient which have been reported in the literature from experiments involving d.c. electric fields. The solution of Eq. (1) is feasible provided the correlation between average electron energy and the applied microwave field has been established.

A study of the electron motion in a microwave field shows that the electron average energy will be modulated in time at a frequency which is twice the microwave frequency. The degree of energy modulation depends upon the ratio of the electron energy relaxation time to the period of oscillation. In air, where the energy losses due to molecular vibrational and rotational inelastic collisions are large compared to the energy losses due to elastic collisions, the electrons lose their energy very rapidly so that the electron energy relaxation time can be comparable and even smaller than the period of oscillation.

At low pressures or short wavelengths, the energy relaxation time is large compared to a period so that the degree of energy modulation is negligible and the electron average energy can be considered as independent of time. In this case, the high frequency field can be replaced by a properly defined effective d.c. field according to

$$E_e = E_{rms}/[1 + (\omega/\nu_c)^2]^{1/2} \simeq E_{rms}/[1 + (36/p_o\lambda)^2]^{1/2} \qquad (2)$$

The term $[1 + (\omega/\nu_c)^2]^{1/2}$ is a measure of the efficiency of energy transfer from the microwave field to the electron. The efficiency of energy transfer decreases as the pressure or wavelength decreases, with the efficiency term becoming important for $p_o\lambda$ less than 200. A plot of E_{rms}/E_e as a function of $p_o\lambda$ is shown in Figure 1. The coefficients in Eq. (1) can be determined directly by considering E_e as an equivalent d.c. field.

For $p_o\lambda$ larger than 250, the energy relaxation time becomes comparable to the period and the degree of energy modulation becomes important. The actual time variation of the electron energy in a given microwave field is determined from a solution of the energy balance equation. The solution of average energy as a function time coupled with the known variation of ν_i, ν_a, and D with average energy determines the time variation of ν_i, ν_a, and D. These functions are now

averaged over time, since it is the average value of the coefficients which is important. The time average of the diffusion coefficient is fairly independent of the degree of energy modulation and can be determined directly from the value of E_e as in the low pressure-wavelength case. However, this is not the situation for the frequencies of ionization and attachment. The time average of $(\nu_i - \nu_a)/p_o$ as a function of E_e/p_o is shown in Figure 2 for various values of $p_o\lambda$. It is observed that the effect of energy modulation is to increase significantly the net average rate of the electron production. This occurs since the ionization rate increases very rapidly with the electron energy so that the peaks of energy in the modulation cycle produce large values of electron ionization. For simplicity, it is desirable to condense these curves to one single curve. This is readily accomplished by normalizing the various curves to the curve corresponding to $p_o\lambda=0$. The transformation is given by

$$(E_e/p_o)n \rightarrow \Delta = E_e/p_o \qquad (3)$$

where Δ, the normalizing factor, is plotted as a function of $p_o\lambda$ in Figure 3. Thus all the curves are reduced to the one curve corresponding to $p_o\lambda = 0$. The value of E_e/p_o corresponding to a given value of $\frac{(\nu_i - \nu_a)}{p_o}$ and $p_o\lambda$ can be obtained by subtracting Δ from the normalized value of E_e/p_o, i.e. the value of E_e/p_o corresponding to $p_o\lambda = 0$.

The most general solution of the continuity equation, Eq. (1) can be written as

$$\ell n(n_b/n_o) = [\langle \nu_i - \nu_a \rangle/p_o + (\nabla^2 Dn)/p_o n]\, p_o t_b \qquad (4)$$

where n_o is the residual electron density produced by external radiation, which may be in the form of a radioactive source near the discharge region, n_b is the electron density at breakdown, and t_b is the time at which breakdown occurs. Eq. (4) is a boundary value problem since the condition that the electron density is zero at the walls of the surrounding vessel must be satisfied. Three distinct breakdown conditions will be treated; breakdown using cw power, breakdown using a single rectangular pulse, and breakdown using rectangular pulses at various repetition frequencies. For discussion sake, the case of breakdown between two infinite parallel plates, separated by a distance d with a uniform electric field will be considered.

A. CW Breakdown

The condition for cw breakdown is that the production of electrons is equal to the loss of electrons and is expressed by the relation

$$\langle \nu_i - \nu_a \rangle + \nabla^2(Dn)/n = o \qquad (5)$$

This is evident from Eq.(4) since the density at breakdown, which has a finite value, is allowed to build up in an infinite time. The solution of Eq. (5) is shown in Figure 4 for the case of infinite parallel plates where the normalized value of E_e/p_o is plotted as a function of the variable $p_o d$, pressure times gap distance. It is seen that for large values of $p_o d$, attachment is the dominant loss mechanism so that the breakdown field becomes independent of the dimensions of the containing vessel. As diffusion becomes important or as the value of Δ changes, the value of E_e/p_o as a function of pressure is not constant but rather increases with decreasing pressure, thus emphasizing the error in the assumption that the power is proportional to the square of the pressure.

Because of the normalization process, the curve for $(E_e/p_o)n$ is independent of $p_o\lambda$. However, the value of E_{rms}/p_o at a given value of $p_o\lambda$ and $p_o d$ is readily computed from Figure 4 by using the curves of Figures 1 and 3.

B. Single Pulse Breakdown

When a pulse of microwave power is applied, the condition that there exists a balance between the electron production and electron loss is no longer valid since the breakdown must occur within a finite time interval. In the case of single pulse breakdown, the power pulse of width τ seconds is applied individually so that there is no influence of one pulse on the succeeding one. For this condition Eq. (4) becomes

$$\ell n(n_b/n_o)/p_o\tau = \langle \nu_i - \nu_a \rangle / p_o + (\nabla^2 Dn)/p_o n \qquad (6)$$

Figure 5 shows the single pulse breakdown curve for the normalized effective field as a function of pressure times pulse width for various values of $p_o d$. It is observed that as $p_o\tau$ decreases the effect of diffusion in removing electrons from the discharge region is minimized. In addition in the limit of high pressure or long pulse width, the pulsed breakdown field approaches the cw value. The ratio of n_b/n_o is assumed to be 10^8 since this ratio yields the best agreement between theory and experiment. Because of the logarithmic nature of the ratio, an order of magnitude change in n_b/n_o changes the breakdown field values by only a percent or so.

C. Multi-Pulse Breakdown

Application of a series of microwave pulses at a given repetition rate can have the effect of lowering the breakdown field below that for the single pulse breakdown. Electrons produced in one pulse, although not sufficient to produce breakdown can increase the initial electron density for the succeeding pulse and eventually a pulse will occur in which breakdown can take place. The condition that such a process is feasible depends on the removal mechanisms of the electrons during the interpulse period. Unfortunately there exists very little information concerning these removal mechanisms in air. Figure 6 shows experimental data[8] of the normalized breakdown field as a function of repetition rate for various pressures using a 0.8 microsecond pulse under conditions of infinite parallel plate geometry. It is seen that there exists a region of breakdown field which is independent of repetition rate, the single pulse breakdown field; a transition to the condition where the repetition rate becomes important; and at higher repetition rates, not shown, the breakdown field would approach the cw value. From 300 to 1000 mm Hg, the breakdown field at 1000 c.p.s. is essentially the same as the single pulse breakdown value. Thus the single pulse breakdown conditions imposes an upper limit on the value of the breakdown field, the cw breakdown conditions places a lower limit on the field, and the multiple breakdown field can be anywhere within these limits depending on the experimental conditions.

IV. EXPERIMENTAL LIMITATIONS

Before proceeding to the computations of the power handling capacities of practical waveguide systems, it is desirable to discuss the effects and limitations of a number of experimental parameters. These factors must be taken into account in any experimental investigation and in proper interpretation of the theoretical breakdown curves to be presented in the following sections.

A. Effects of Pulse Shape on Breakdown

In developing the theory of pulsed breakdown, it has been assumed that the pulses of microwave power are rectangular in shape. In practice, such is not the case. However, most pulses can be represented to the first approximation as trapezoidal in shape. A typical envelope of a microwave pulse is shown in Figure 7 as the solid line. The equivalent trapezoid used to approximate this pulse is represented by the dotted line. The hatched portion represents the portion of the pulse which will contribute to breakdown; i.e. that portion of the pulse in which the electric field is larger than the cw value. Calculations show that for t_1/t_2 and t_3/t_2 less than one, the trapezoid pulse may be replaced by an equivalent rectangular pulse of width t_2 seconds. For example, the equivalent rectangular pulse in Figure 7 is 0.8 microseconds. Therefore, in interpreting the theoretical breakdown curves, the equivalent rectangular pulse width of the power pulse should be used. In general, for more complicated pulse shapes, the value of the breakdown field must be computed numerically from Eq. (1). For this case, a definition of pulse width is no longer applicable and each case of breakdown must be computed individually.

The calculations of peak power from average power measurements involves a different definition of pulse width. For an arbitrary pulse shape the relation between average power and peak power is given by

$$P_{average} = \text{repetition rate} \times \int P_{peak}\, dt \qquad (7)$$

The peak power is integrated over the time of the pulse. For the trapezoidal pulse, the time $[t_2 + (t_1 + t_3)/2]$ is the corresponding rectangular pulse width which is used in interpreting the power measurements. In Figure 7, the actual area under the pulse was measured yielding a pulse width of one microsecond to be used in the calculation of peak power. This differentiation in the definition of pulse width must be considered for proper interpretation of the experimental measurements.

B. Effects Of An Extemal Radioactive Source On Breakdown

A sufficiently strong radioactive source is necessary in order to insure that a sufficient number of electrons are present in the discharge region so that the statistical fluctuations in the breakdown field are minimized. In the experiments at Microwave Associates, Inc. a radioactive source of cobalt 60, 80 millicurie in strength, was used. A typical curve of the sparking probability, i.e. the number of breakdowns per pulse, as a function of relative incident power for various values of lead thickness between the source and the discharge region is shown in Figure 8. The conditions of the measurements are atmospheric pressure, 0.8 microsecond pulse width, and 1000 c.p.s. repetition rate. The number of breakdowns is determined from the number of light impulses detected by a photomultiplier which are counted on a standard Berkeley counter. This work and the results reported by Cooper[9] demonstrate that the sparking probability is a function of the irradiation conditions of the discharge region and microwave field, whereas, there exists a threshold value of breakdown field which is fairly insensitive to the irradiation conditions. The theoretical pulsed breakdown field represents the minimum field necessary for breakdown and, consequently, is associated with the threshold value of breakdown. Rather than establishing the threshold field from curves as shown in Figure 8, which can present a tedious task, the threshold field can be

assumed when a sparking probability of 10^{-3} exists. Thus a strong radioactive source is desirable in order to eliminate the necessity of determining sparking probability curves for every experimental condition and to enhance the accuracy and reproducibility of the threshold field measurements.

C. Effects Of Temperature and Altitude On Breakdown

All gas pressures used in the computation of breakdown electric field values must be referred to 20°C (293°K). Since the mechanisms controlling breakdown depend upon gas density, it was necessary to normalize the pressure to some convenient reference temperature. For any given condition of pressure, p, and temperature, T(°K), the pressure normalized to 20°C, p_o, is readily computed from the expression

$$p_o = (293/T)p \tag{8}$$

In considering the pressure corresponding to a given altitude above sea level, it is necessary to correct for the change in gas temperature with altitude. Figure 9 shows pressure, normalized to 20°C, as a function of altitude [10]. The correction for the decrease in gas temperature as the altitude increases has been included in Figure 9.

D. Variation of Breakdown Power with Voltage Standing Wave Ratio

The breakdown power capacities are computed on the assumption that no standing waves exist in the section of waveguide of interest. The presence of a standing wave, and hence a mismatch, will deteriorate the power handling capacity of the system. The relation between the actual breakdown power, P, and the breakdown power for a matched waveguide system, P_m, as a function of voltage standing wave ratio, VSWR, is given by

$$P_m/P = [2\,VSWR/(VSWR + 1)]^2 \tag{9}$$

This relationship is plotted in Figure 10. The breakdown power computed in the following sections must be corrected for any standing waves present in the discharge region according to Eq. (9).

E. Variation of Breakdown Power With Repetition Rate

The breakdown powers for both cw and single pulse conditions for the various waveguide systems are computed in the following sections. A quantitative treatment of the effect of repetition rate on breakdown power is not available because of the lack of information concerning the interpulse electron removal mechanisms. However, the single pulse breakdown condition imposes an upper limit on the breakdown power whereas the cw breakdown condition imposes a lower limit on the breakdown power. Measurements of breakdown power as a function of repetition rate indicate that there exists a wide range of repetition rates in which the single pulse breakdown conditions are valid. This range of repetition rate is given approximately by the condition that the repetition rate be less than three times the pressure. Figure 11 shows the region of repetition rate in which the single pulse breakdown conditions are valid. For the region where single pulse breakdown conditions are not valid, the variation of breakdown power with repetition rate must be determined experimentally in order to obtain an accurate value of breakdown power.

V. RECTANGULAR WAVEGUIDES

The breakdown power as a function of operating parameters will be considered for the rigid rectangular waveguide operating in the dominant or TE_{10} mode. The electric field configuration for this mode in terms of the r.m.s. field is

$$E = E_{rms}\cos(\pi x/a) \tag{10}$$

The maximum field intensity is parallel to the narrower dimension of the guide, midway between the side walls and is independent of the distance from the wide faces of the guide. The relation between the power carried by the waveguide and the maximum r.m.s. electric field is

$$P = 1.33 \times 10^{-3}(ab)(\lambda/\lambda_g)(E_{rms})^2 \tag{11}$$

If the field E_{rms} is expressed in volt/cm and the dimensions of the guide, a and b, are expressed in centimeters, the power, P, is obtained in watts. The guide wavelength is given by

$$\lambda_g = \lambda/[1-(\lambda/\lambda_c)^2]^{1/2} \tag{12}$$

where λ_c, the cut-off wavelength, is equal to 2a. A plot of λ/λ_g as a function of λ/λ_c is shown in Figure 12. Curves for computing breakdown power will be given for different ratios of a/b. The following will be considered:

1) Full height waveguide; a/b equal to 2
2) Half height waveguide; a/b equal to 4
3) Narrow height waveguide; a/b greater than 8

The conditions of breakdown are determined from a solution of the following differential equation obtained from the continuity equation, Eq. (4)

$$\ell n(n_i/n_o)/p_o\tau = \langle\nu_i-\nu_a\rangle/p_o + \left[\frac{\partial^2(Dn)}{\partial x^2} + \frac{\partial^2(Dn)}{\partial y^2}\right]/p_o n \tag{13}$$

The coefficient ν_i, ν_a, and D are functions of position in space since the electric field is a function of position according to Eq. (10). Eq. (13) is solved subject to the boundary conditions that the electron density vanish along the inside walls of the waveguide.

The solution of Eq. (13) yields the ratio of normalized effective breakdown field to pressure as a function of experimental parameters. The normalized effective breakdown field is transformed to the corresponding r.m.s. field by applying the correction for energy modulation according to Eq. (3) and Figure 3 and the correction for efficiency of energy transfer according to Eq. (2) and Figure 1. These corrections depend on the product of pressure times wavelength so that the power, given by Eq. (1), depends on frequency not only through the term (λ/λ_g) but also through the r.m.s. field. In comparing the various waveguide sizes, it is more convenient to transform Eq. (11) to the following form

$$P(\lambda_g/\lambda)/ab(p_o)^2 = 1.33 \times 10^{-3}(E_{rms}/p_o)^2 = K \tag{14}$$

For a given waveguide size, K will be a function of frequency because of the frequency dependence of E_{rms}. Therefore, in presenting values of K at breakdown as a function of experimental parameters, the mid-band frequency of the particular waveguide is used in the calculations. The data will be presented so that the breakdown power can be computed for any frequency over the operating range of the waveguide and for any particular experimental conditions.

A. CW Breakdown Power

The solution of Eq. (13) for the condition of cw breakdown is shown in Figure 13. The ratio of normalized cw breakdown field to pressure is plotted as a function of pressure times the height of the waveguide for values of a/b equal to 2, 4, and greater than 8. From Figure 13 and Eqns. (2), (3), and (11), the cw breakdown power can be computed for all rectangular waveguides as a function of pressure. Table I shows the list of the RETMA standard for rigid rectangular waveguides. Included are the frequency range for the dominant TE_{10} mode, the waveguide inside dimensions, the cut-off wavelength of the TE_{10} mode, and the cw power rating at atmospheric pressure for the lowest and the highest frequency. The cw breakdown power in terms of K is plotted as a function of pressure in Figure 14. The curves for the most common waveguides at midband frequency are shown. It is obvious from Figure 14 that the ratio of breakdown power to pressure, P/p_o^2, is not constant as a function of pressure. The deviation becomes especially important at higher frequencies and at lower pressures. The assumption that breakdown measurements taken at low pressures in a given waveguide system can be extrapolated to higher pressures by assuming P/p_o^2 constant will lead to erroneous values for the higher pressure breakdown power. Any particular waveguide size and frequency not included in Figure 14 can be computed directly from Figure 13. Typical examples of the computation for breakdown power will be given in a following section.

B. Pulsed Breakdown Power

The solution of Eq. (13) for the condition of single pulse breakdown is shown in Figures 15 and 16. The ratio of the normalized single pulse breakdown field to pressure is plotted as a function of pressure times pulse width for various values of pressure times waveguide height. Figure 15 corresponds to the condition of a/b equal to two and Figure 16 corresponds to the condition of a/b greater than 8. The curve for a/b equal to four is not shown but can be computed by interpolation from Figures 15 and 16. A value of n_i/n_o equal to 10^8 is used in computing Figures 15 and 16. This value implies a rather large external radioactive source in the vicinity of the discharge region, however, even in the case of no external source it includes breakdown due to occasional large bursts of cosmic radiation. The single pulse breakdown power in terms of K is plotted as a function of pressure for a pulse width of one microsecond in Figure 17. The breakdown power for any other pulse width can be computed directly from Figure 15. Figure 18 shows the single pulse breakdown power in terms of K as a function of pulse width at atmospheric pressure. These curves are different for other values of pressure. The curves for WR-187, WR-284, and WR650 are identical and the factor K is independent of frequency for these three waveguides.

C. Numerical Examples Of The Breakdown Power Calculations

Examples of the procedure to follow in computing the breakdown power for a given set of conditions will be presented by outlining in detail the solution of a number of typical problems for each waveguide system.

1) Problem: Compare the single pulse breakdown power of WR-112 and WR-90 waveguides at 40 mm Hg using a rectangular power pulse of 1/2 microsecond pulse width and a frequency of 9000 megacycles/sec at 20°C.

Solution: The solution for each waveguide will be considered separately but tabulated side by side.

		WR-112	WR-90
a) Using Table I compute the following quantities	(ab)	3.59	2.33
	(λ/λ_c)	0.584	0.728
	$p_o b$	50.5	40.8
	$p_o \lambda$	133	133
	$p_o r$	2×10^{-5}	2×10^{-5}
b) From Figure 12 determine	(λ/λ_g)	0.810	0.682
c) From Figure 15 determine	$(E_e/p_o)n$	51	51
d) From Figure 3 determine and using Eq. (3)	Δ	0.5	0.5
	E_e/p_o	50.5	50.5
e) Multiply by p_o to obtain	E_e	2020	2020
f) From Figure 1 determine and compute	E_{rms}/E_e	1.03	1.03
	E_{rms}	2080	2080
g) From Eq. (11) compute	P	16.7 kw	9.2 kw

For the conditions of the problem the breakdown power of WR-112 is 16.7 kilowatts and the breakdown power of WR-90 is 9.2 kilowatts.

2) Problem: Compare the cw breakdown power of WR-187 for both full height and half height waveguide at 5000 megacycles/sec. The pressure is 20 mm Hg at 100°C.

Solution: The solution for each case will be considered separately but tabulated side by side.

		Full Height	Half Height
a) Normalize the pressure according to Eq. (6) to 20°C	p_o	15.7	15.7
b) Using Table I compute the following quantities	(ab)	10.5	5.25
	(λ/λ_c)	0.632	0.632
	$p_o b$	34.8	17.4
	$p_o \lambda$	95	95
c) From Figure 12 determine	(λ/λ_g)	0.773	0.773
d) From Figure 13 determine	$(E_e/p_o)n$	33	34.5

		Full Height	Half Height
e) From Figure 3 determine	Δ	0.3	0.3
and using Eq. (3)	E_e/p_o	32.7	34.2
f) Multiply by p_o to obtain	E_e	514	527
g) From Figure 1 determine	E_{rms}/E_e	1.07	1.07
and compute	E_{rms}	550	575
h) From Eq. (10) compute	P	3.25 kw	1.78 kw

For the conditions of the problem the breakdown power for full height guide is 3.25 kilowatts and for half height guide 1.78 kilowatts.

3) Problem: Compute the single pulse breakdown power of WR-19 waveguide operating at 1600 mm Hg and 20°C using a rectangular power pulse of 0.1 microsecond in width and a frequency of 50,000 megacycles/sec.

Solution:		WR-19
a) Using Table I, compute the	(ab)	0.116
following quantities	λ/λ_c	0.615
	$p_o b$	384
	$p_o \lambda$	960
	$p_o f$	1.6×10^{-4}
b) From Figure 12 determine	λ/λ_g	0.79
c) From Figure 15 determine	$(E_e/p_o)n$	37.3
d) From Figure 3 determine	Δ	3.7
and using Eq. (3)	E_e/p_o	33.6
e) From Figure 1 determine	E_{rms}/E_e	1
f) Multiply by p_o to obtain	E_{rms}	53,800
g) From Eq. (10) compute	P	354 kw

Thus the single pulse breakdown power for the above conditions in WR-19 waveguide is 354 kilowatts.

VI. COAXIAL WAVEGUIDES

The breakdown power as a function of operating parameters will be considered for the rigid coaxial waveguide operating in the dominant or TEM mode. The electric field configuration for this mode in terms of the r.m.s. field is

$$E = E_{rms}(r_1/r) \tag{15}$$

The maximum field intensity occurs at the inner conductor radius, r_1, and is represented by E_{rms}.

The relation between the power carried by the waveguide and the maximum r.m.s. electric field is

$$P = (r_1)^2 \ln(r_2/r_1)\,(E_{rms})^2/30 \qquad (16)$$

The calculations of breakdown field are performed for coaxial systems having an impedance of 50 ohms. This corresponds to a ratio of outer conductor to inner conductor, r_2/r_1, of 2.3. The conditions of breakdown are determined from a solution of the following differential equation obtained from the continuity equation, Eq. (4)

$$\ell n(n_b/n_o)/p_o\tau = \langle \nu_i - \nu_a \rangle/p_o + \left[\frac{1}{r}\,\frac{\partial}{\partial r}\left(\frac{r\,2(D_n)}{2r}\right)\right]/p_o n \qquad (17)$$

The coefficients ν_i, ν_a, and D are functions of radius since the electric field varies according to Eq. (15). Eq. (17) is solved subject to the boundary conditions that the electron density vanish along the walls of the inner and outer conductor. The solution of Eq. (17) yields the ratio of normalized effective breakdown field to pressure as a function of experimental parameters. In comparing the breakdown power of the various coaxial sizes, it is more convenient to transform Eq. (16) to the following form

$$P/(p_o r_o)^2 = .0278(E_{rms}/p_o)^2 = K \qquad (18)$$

For each coaxial size, K will be computed for a typical frequency. The data will be presented so that the breakdown power can be computed for any frequency over the operating range of the coaxial waveguide and for any particular experimental conditions.

A. CW Breakdown Power

The solution of Eq. (17) for the condition of cw breakdown is shown in Figure 19. The ratio of normalized cw breakdown field to pressure is shown as a function of pressure times inner conductor radius for a ratio r_2/r_1 equal to 2.3. From Figure 19 and Eqns. (2), (3), and (16), the cw breakdown power can be computed for all coaxial waveguides of 50 ohm impedance as a function of pressure. Table II shows the list of standard coaxial waveguides. Included are the frequency range for the dominant TEM mode, the inner and outer conductor dimensions and the cw power rating at atmospheric pressure. The cw breakdown power in terms of K is plotted as a function of pressure in Figure 20. The curves for the most common coaxial sizes and typical frequencies are shown. Any particular coaxial size and frequency not included in Figure 20 can be computed directly from Figure 19. Typical examples of the calculation for breakdown power will be given in a following section.

B. Pulsed Breakdown Power

The solution of Eq. (17) for the condition of single pulse breakdown is shown in Figure 21. The ratio of the normalized single pulse breakdown field to pressure is plotted as a function of pressure times pulse width for various values of pressure times inner conductor radius. A value of n_b/n_o equal to 10^3 is used in computing Figure 21. The single pulse breakdown power in terms of K for the most common coaxial systems is plotted as a function of pressure for a pulse width of one microsecond in Figure 22. The breakdown power for any other pulse width can be

computed directly from Figure 21. Figure 23 shows the single pulse breakdown power in terms of K as a function of pulse width at atmospheric pressure. These curves are different for other values of pressure. The curves for RG153/U, RG154/U, and RG152/U are identical and the factor K is independent of frequency for these three coaxial waveguides. These curves represent typical operation under normal pulsed conditions.

C. Numerical Examples Of The Breakdown Power Calculations

1) Problem: Compute the cw breakdown power of RG154/U coaxial waveguide operating at 100 mm Hg and 20°C and at a frequency of 1000 megacycles/sec.

Solution:		RG154/U
a) Using Table II compute the following quantities	r_1	3.30
	$p_o r_1$	167
	$p_o \lambda$	3000
b) From Figure 19 determine	$(E_e/p_o)n$	33.8
c) From Figure 3 determine and using Eq. (3)	Δ	5.5
	(E_e/p_o)	28.3
d) Multiply by p_o to obtain	E_e	2830
e) From Figure 1 determine and hence	E_{rms}/E_e	1
	E_{rms}	2830
f) From Eq. (16) or (18) compute	P	625 kw

For the conditions of the problem the cw breakdown power of RG154/U coaxial waveguide is 625 kilowatts.

2) Problem: Compute the single pulse breakdown power of RG151/U coaxial waveguide operating at 760 mm Hg and -15°C and using a rectangular power pulse of 2 microseconds in width and a frequency of 9000 megacycles/sec.

Solution:		RG151/U
a) Normalize the pressure according to Eq. (8) to 20°C	p_o	860
b) Using Table II compute the following quantities	r_1	0.159
	$p_o r_1$	137
	$p_o \lambda$	2800
	$p_o r$	1.72×10^{-3}
c) From Figure 21 determine	$(E_e/p_o)n$	35.8
d) From Figure 3 determine and using Eq. (3)	Δ	5.4
	E_e/p_o	30.4
e) Multiply by p_o to obtain	E_e	26,200

f) From Figure 1 determine	E_{rms}/E_e	1
and hence	E_{rms}	26,200
g) From Eq. (16) or (18) compute	P	490 kw

The single pulse breakdown power for the above conditions in RG151/U coaxial waveguide is 490 kilowatts.

VII. CIRCULAR WAVEGUIDE - TE_{11} MODE

The breakdown power as a function of operating parameters will be considered for the rigid circular waveguide operating in the dominant or TE_{11} mode. The electric field configuration for this mode in terms of the maximum r.m.s. field is

$$E_r = E_{rms}\left[\frac{2J_1(1.84r/r_o)}{(1.84r/r_o)}\right]\sin\theta$$

$$E_\theta = E_{rms}\left[J_o(1.84r/r_o) - J_2(1.84r/r_o)\right]\cos\theta \qquad (19)$$

where r_o is the radius of the circular conductor. The electric field has components in the radial direction, E_r, and in the angular direction, E_θ, and is a function of radius and angle within the circular cross-section. For simplicity in solving the continuity equation, the angular dependence of the electric field is removed by considering the electric field to be averaged over angle. With this assumption the magnitude of the electric field at a given radius is expressed by

$$E = \frac{E_{rms}}{1.41}\left\{\left[\frac{2J_1(1.84r/r_o)}{1.84r/r_o}\right]^2 + \left[J_o(1.84r/r_o) - J_2(1.84r/r_o)\right]^2\right\}^{1/2} \qquad (20)$$

The relation between the power carried by the waveguide and the maximum r.m.s. electric field is

$$P = 3.98 \times 10^{-3}(r_o)^2(\lambda/\lambda_g)(E_{rms})^2 \qquad (21)$$

The guide wavelength is determined from Eq. (12) and the cut-off wavelength for this mode is λ_c equal to $3.41r_o$.

The conditions of breakdown are determined from a solution of the continuity equation, given by Eq. (17), subject to the boundary condition that the electron density vanish along the inside walls of the circular guide. The coefficients ν_i, ν_a, and D are functions of radius because of the radial variation of the electric field as determined by Eq. (21). In comparing the breakdown power of the various cylindrical waveguide sizes, it is more convenient to transform Eq. (21) to the following form

$$P(\lambda_g/\lambda)/(p_o r_o)^2 = 3.98 \times 10^{-3}(E_{rms}/p_o)^2 = K \qquad (22)$$

For each cylindrical waveguide, K will be computed for the midband frequency.

A. CW Breakdown Power

The solution of Eq. (17) for the condition of cw breakdown is shown in Figure 24. The

ratio of normalized cw breakdown field to pressure is plotted as a function of pressure times conductor radius. From Figure 24 and Eqns. (2), (3), and (21), the cw breakdown power can be computed as a function of pressure for all circular waveguide sizes. Table III shows the list of common waveguide sizes for TE_{11} operation. These waveguide sizes have recently been standardized by the RETMA. Included in the table are the frequency range for TE_{11} operation, the waveguide dimension, the cut-off wavelength, and the cw power rating at atmospheric pressure. The cw breakdown power in terms of K is plotted as a function of pressure in Figure 25. The curves for the common cylindrical sizes and midband frequencies are shown. Any particular cylindrical size and frequency not included in Figure 25 can be computed directly from Figure 24.

B. Pulsed Breakdown Power.

The solution of Eq. (17) for the condition of single pulse breakdown is shown in Figure 26. The ratio of normalized single pulse breakdown field to pressure is plotted as a function of pressure times pulse width for various values of pressure times conductor radius. A value of n_b/n_o equal to 10^8 is used in computing in Figure 26. The single pulse breakdown power in terms of K for the common cylindrical waveguides is plotted as a function of pressure for a pulse width of one microsecond in Figure 27. The breakdown power for any other pulse width can be computed directly from Figure 26. Figure 28 shows the single pulse breakdown power in terms of K as a function of pulse width at atmospheric pressure. These curves represent typical operation under normal pulsed conditions.

C. Numerical Examples of the Breakdown Power Calculations

1) Problem: Compare the cw and single pulse breakdown powers of WC-28 circular waveguide operating in the TE_{11} mode at 24 kilomegacycles/sec. The power pulse is .1 microsecond pulse width and the pressure is 300 mm Hg at 20°C.

Solution: The solution for each condition will be considered separately but tabulated side by side

		CW	Single Pulse
a) Using Table III compute	r_o	.356	.356
the following quantities	λ/λ_c	.768	.768
	$p_o r_o$	107	107
	$p_o \lambda$	375	375
	$p_o \tau$		3×10^{-5}
b) From Figure 12 determine	λ/λ_g	.64	.64
c) From Figures 24 and 26 determine	$(E_e/p_o)n$	31.8	47.3
d) From Figure 3 determine	Δ	1.4	1.4
and using Eq. (3)	E_e/p_o	30.4	45.9
e) Multiply by p_o to obtain	E_e	9,100	13,800
f) From Figure 1 determine	E_{rms}/E_e	1	1
and compute	E_{rms}	9,100	13,800
g) From Eq. (21) compute	P	26.4 kw	61 kw

For the conditions of the problem, in WC-28 circular waveguide the cw breakdown power is 26.4 kilowatts and the single pulse breakdown power is 61 kilowatts.

2) Problem: Compute the cw breakdown power for WC-59 waveguide at a pressure of 760 mm Hg for temperatures of 20°C and 200°C. The frequency is 16,000 megacycles/sec.

Solution:		20°C	200°C
a) Normalize the pressure according to Eq. (8) to 20°C	p_o	760	470
b) Using Table III compute the following quantities	r_o	.754	.754
	(λ/λ_c)	.73	.73
	$p_o r_o$	572	354
	$p_o \lambda$	1420	880
c) From Figure 12 determine	λ/λ_g	.68	.68
d) From Figure 24 determine	$(E_e/p_o)_a$	31.5	31.5
e) From Figure 3 determine	Δ	4.4	3.4
and using Eq. (3)	E_e/p_o	27.1	28.1
f) Multiply by p_o to obtain	E_e	20,600	13,200
g) From Figure 1 determine	E_{rms}/E_e	1	1
and compute	E_{rms}	20,600	13,200
h) From Eq. (21) compute	P	650 kw	267 kw

For the conditions of the problem in WC-59 circular waveguide the cw breakdown power at 20°C is 650 kilowatts and at 200°C is 267 kilowatts.

VIII. CIRCULAR WAVEGUIDE - TE_{01} MODE

The breakdown power as a function of operating parameters will be considered for the rigid circular waveguide operating in the TE_{01} mode. The electric field configuration for this mode in terms of the maximum r.m.s. field is

$$E = (E_{rms}/.582)J_1(3.83r/r_o) \qquad (23)$$

The electric field is directed perpendicular to the radial direction and has a null at the center of the waveguide and at the walls. The maximum field intensity occurs at a value of radius equal to 0.48 times the conductor radius. The relation between the power carried by the waveguide and the maximum r.m.s. electric field is

$$P = 3.98 \times 10^{-3} (r_o)^2 (\lambda/\lambda_g)(E_{rms})^2 \qquad (24)$$

The guide wavelength is determined from Eq. (12) and the cut-off wavelength for this mode is λ_c equal to $1.64 r_o$.

The conditions of breakdown are determined from a solution of the continuity equation,

given by Eq. (17) subject to the boundary condition that the electron density vanish along the inside walls of the circular waveguide. The coefficients ν_i, ν_a, and D are functions of radius because of the radial variation of the electric field as determined by Eq. (23). In comparing the breakdown power of the various cylindrical waveguide sizes, it is more convenient to transform Eq. (24) to the form of Eq. (22). For each cylindrical waveguide, K will be computed for the midband frequency.

A. CW Breakdown Power

The solution of Eq. (17) for the condition of cw breakdown is shown in Figure 29 where the ratio of normalized cw breakdown field to pressure is plotted as a function of pressure times conductor radius. Table IV shows the list of common waveguide sizes for TE_{01} operation which have recently been standardized by the RETMA. Included in the table are the frequency range for TE_{01} operation, the waveguide dimensions, the cut-off wavelength, and the cw power rating at atmospheric pressure. The cw breakdown power in terms of K is plotted as a function of pressure in Figure 30. The curves for the common cylindrical sizes and midband frequencies are shown.

B. Pulsed Breakdown Power

The solution of Eq. (17) for the condition of single pulse breakdown is shown in Figure 31 where the ratio of normalized single pulse breakdown field to pressure is plotted as a function of pressure times pulse width for various values of pressure times conductor radius. The single pulse breakdown power in terms of K for the common cylindrical waveguides at the midband frequency is plotted as a function of pressure for a pulse width of one microsecond in Figure 32. Figure 33 shows the single pulse breakdown power in terms of K as a function of pulse width at atmospheric pressure.

IX. CIRCULAR WAVEGUIDE - TM_{01} MODE

The breakdown power as a function of operating parameters will be considered for the rigid circular waveguide operating in the TM_{01} mode. The electric field configuration for this mode in terms of the maximum r.m.s. field is

$$\begin{aligned} E_z &= E_{rms}\, J_o(2.405 r/r_o) \\ E_r &= E_{rms}\, (\lambda_c/\lambda_g) J_1(2.405 r/r_o) \end{aligned} \tag{25}$$

The electric field has components along the axis of the waveguide, E_z, and in the radial direction, E_r. For normal TM_{01} mode operation, the condition that r_o/λ is less than 0.76 is satisfied so that the electric field which controls breakdown is directed along the waveguide axis, i.e. E_z. For this case, the maximum field intensity occurs in the center of the guide. The relation between the power carried by the waveguide and the maximum r.m.s. electric field is

$$P = 15.4 \times 10^{-3} (\lambda/\lambda_g)(r_o^4/\lambda^2)(E_{rms})^2 \tag{26}$$

The guide wavelength is determined from Eq. (12) and the cut-off wavelength for this mode is λ_c equal to $2.87 r_o$.

The conditions of breakdown are determined from a solution of the continuity equation, given by Eq. (17), subject to the boundary condition that the electron density vanish along the

inside walls of the circular guide. In comparing the breakdown power of the various waveguide sizes, it is convenient to transform Eq. (26) to the following form

$$P(\lambda_g/\lambda)\,(\lambda/r_o)^2/(p_o/r_o)^2 = 15.4 \times 10^{-3}(E_{rms}/p_o)^2 = K \qquad (27)$$

For each cylindrical waveguide, K will be computed for a typical frequency of operation.

A. CW Breakdown Power

The solution of Eq. (17) for the condition of cw breakdown is shown in Figure 34 where the ratio of normalized cw breakdown field to pressure is plotted as a function of pressure times conductor radius. As yet the circular waveguide sizes for TM_{01} operation have not been standardized by the RETMA. Table V shows a list of common waveguide sizes for TM_{01} operation with typical operating frequencies. The waveguide dimensions, cut-off wavelength, and the cw power rating at atmospheric pressure are included in the table. The cw breakdown power in terms of K is plotted as a function of pressure in Figure 35. The curves for the common cylindrical sizes and typical frequencies are shown.

B. Pulsed Breakdown Power

The solution of Eq. (17) for the condition of single pulse breakdown is shown in Figure 36 where the ratio of normalized single pulse breakdown field to pressure is plotted as a function of pressure times pulse width for various values of pressure times conductor radius. The single pulse breakdown power in terms of K for the common waveguides at typical frequencies is plotted as a function of pressure for a pulse width of one microsecond in Figure 37. Figure 38 shows the single pulse breakdown power in terms of K as a function of pulse width at atmospheric pressure.

TABLE I

STANDARD RECTANGULAR WAVEGUIDES

Dimensions and Wave Properties

RETMA DESIGNATION	FREQUENCY RANGE (kmc/s)		INSIDE DIMENSIONS (inches)		INSIDE DIMENSIONS (centimeter)		CUT-OFF WAVELENGTH (cm)	CW BREAKDOWN POWER-760 mm Hg (megawatts)	
			WIDTH	HEIGHT	WIDTH	HEIGHT			
	f_1	f_2						f_1	f_2
WR770	0.96	1.45	7.70	3.85	19.6	9.78	39.1	57.5	81.5
WR650	1.12	1.70	6.50	3.25	16.5	8.26	33.0	40.2	58.0
WR510	1.45	2.20	5.10	2.55	12.9	6.48	25.9	25.3	35.8
WR430	1.70	2.60	4.30	2.15	10.9	5.46	21.8	17.5	25.2
WR340	2.20	3.30	3.40	1.70	8.64	4.32	17.3	11.5	16.0
WR284	2.60	3.95	2.84	1.34	7.21	3.40	14.4	7.30	10.4
WR229	3.30	4.90	2.29	1.14	5.82	2.91	11.6	5.30	7.30
WR187	3.95	5.85	1.87	.872	4.76	2.22	9.51	3.20	4.50
WR159	4.90	7.05	1.59	.795	4.04	2.02	8.08	2.70	3.50
WR137	5.85	8.20	1.37	.622	3.49	1.58	6.97	1.90	2.50
WR112	7.05	10.0	1.12	.497	2.85	1.26	5.70	1.24	1.64
WR90	8.20	12.4	.900	.400	2.29	1.02	4.57	.730	1.10
WR75	10.0	15.0	.750	.375	1.91	.953	3.81	.600	.860
WR62	12.4	18.0	.622	.311	1.58	.790	3.16	.440	.600
WR51	15.0	22.0	.510	.255	1.30	.648	2.59	.300	.410
WR42	18.0	26.5	.420	.170	1.07	.432	2.13	.160	.240
WR34	22.0	33.0	.340	.170	.866	.432	1.73	.130	.185
WR28	26 5	40.0	.280	.140	.711	.356	1.42	.095	.145
WR22	33.0	50.0	.224	.112	.569	.284	1.14	.062	.090
WR19	40.0	60.0	.188	.094	.487	.239	.974	.047	.064
WR15	50.0	75.0	.148	.074	.376	.188	.752	.029	.042
WR12	60.0	90.0	.122	.061	.310	.155	.620	.020	.029
WR10	75.0	110	.100	.050	.254	.127	.508	.014	.020

TABLE II

STANDARD COAXIAL WAVEGUIDES

Dimensions and Wave Properties

WAVEGUIDE TYPE	FREQUENCY RANGE (mc/s)		IMPEDANCE (ohms)	OUTER CONDUCTOR DIAMETER (inches)	INNER CONDUCTOR RADIUS (cm)	CW BREAKDOWN POWER-760 mm Hg (megawatts) at f_2
	f_1	f_2				
RG152/U	.5	650	50	6.13	3.30	110
RG154/U	.5	1,300	50	3.13	1.67	29
RG153/U	.5	2,700	50	1.61	.843	7.35
RG155/U	.5	3,300	50	.875	.432	2.10
RG151/U	.5	10,000	50	.375	.159	.350

TABLE III

STANDARD CIRCULAR WAVEGUIDES

Dimensions and Wave Properties for TE_{11} Mode

RETMA DESIGNATION	FREQUENCY RANGE (kmc/sec)		INSIDE DIAMETER (inches)	INSIDE RADIUS (cm)	CUT-OFF WAVELENGTH (cm)	CW BREAKDOWN POWER-760 mm Hg (megawatts)	
	f_1	f_2				f_1	f_2
WC-94	8.49	11.6	.938	1.19	4.06	1.1	1.78
WC-59	13.4	18.4	.594	.754	2.57	.46	.75
WC-38	21.2	29.1	.375	.476	1.62	.19	.33
WC-28	28.3	38.8	.281	.356	1.21	.11	.19
WC-14	56.6	77.5	.141	.179	.610	.033	.053

TABLE IV

STANDARD CIRCULAR WAVEGUIDES

Dimensions and Wave Properties for TE_{01} Mode

RETMA DESIGNATION	FREQUENCY RANGE (kmc/sec)		INSIDE DIAMETER (inches)	INSIDE RADIUS (cm)	CUT-OFF WAVELENGTH (cm)	CW BREAKDOWN POWER-760 mm Hg (megawatts)	
	f_1	f_2				f_1	f_2
WC-240	7.25	9.98	2.403	3.055	5.01	8.1	12
WC-128	13.6	18.7	1.281	1.63	2.67	2.45	3.6
WC-94	18.6	25.6	.938	1.19	1.95	1.35	2.1
WC-59	29.3	40.4	.594	.754	1.235	.59	.89
WC-33	53.1	73.1	.328	.416	.682	.20	.29

TABLE V

STANDARD CIRCULAR WAVEGUIDES

Dimensions and Wave Properties for TM_{01} Mode

BAND DESIGNATION	FREQUENCY (mc/sec)	INSIDE DIAMETER (inches)	INSIDE RADIUS (cm)	CUT-OFF WAVELENGTH (cm)	CW BREAKDOWN POWER-760 mm Hg (Megawatts)
K	9,375	1.165	1.48	3.87	1.63
K_u	16,000	.683	.867	2.26	.58
K	24,000	.455	.578	1.51	.28
K_a	35,000	.312	.396	1.03	.14
4 mm	70,000	.156	.198	.517	.038

LIST OF ILLUSTRATIONS

LIST OF ILLUSTRATIONS

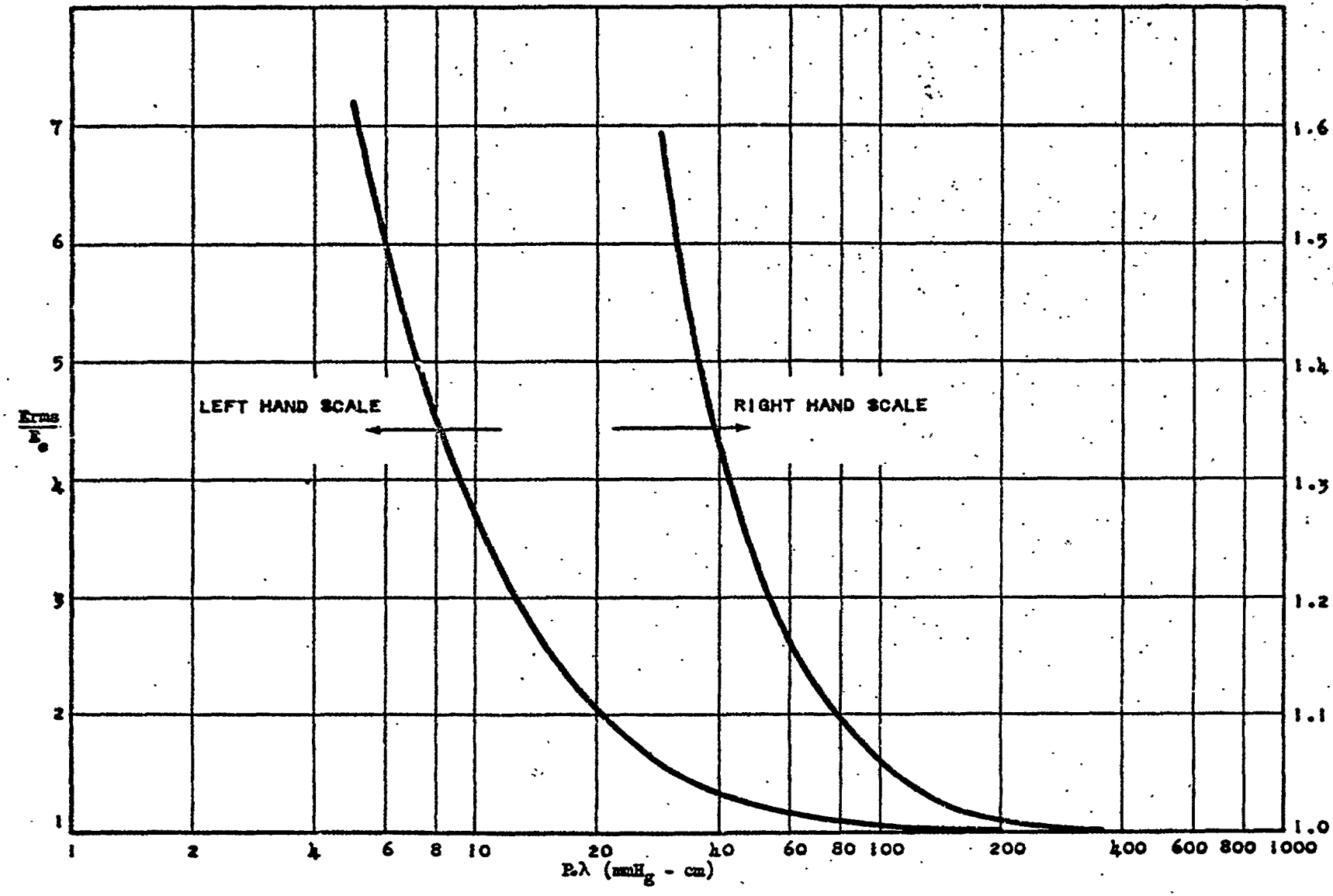

Fig. 1 Ratio of rms to effective value of electric field as a function of pressure times wavelength.

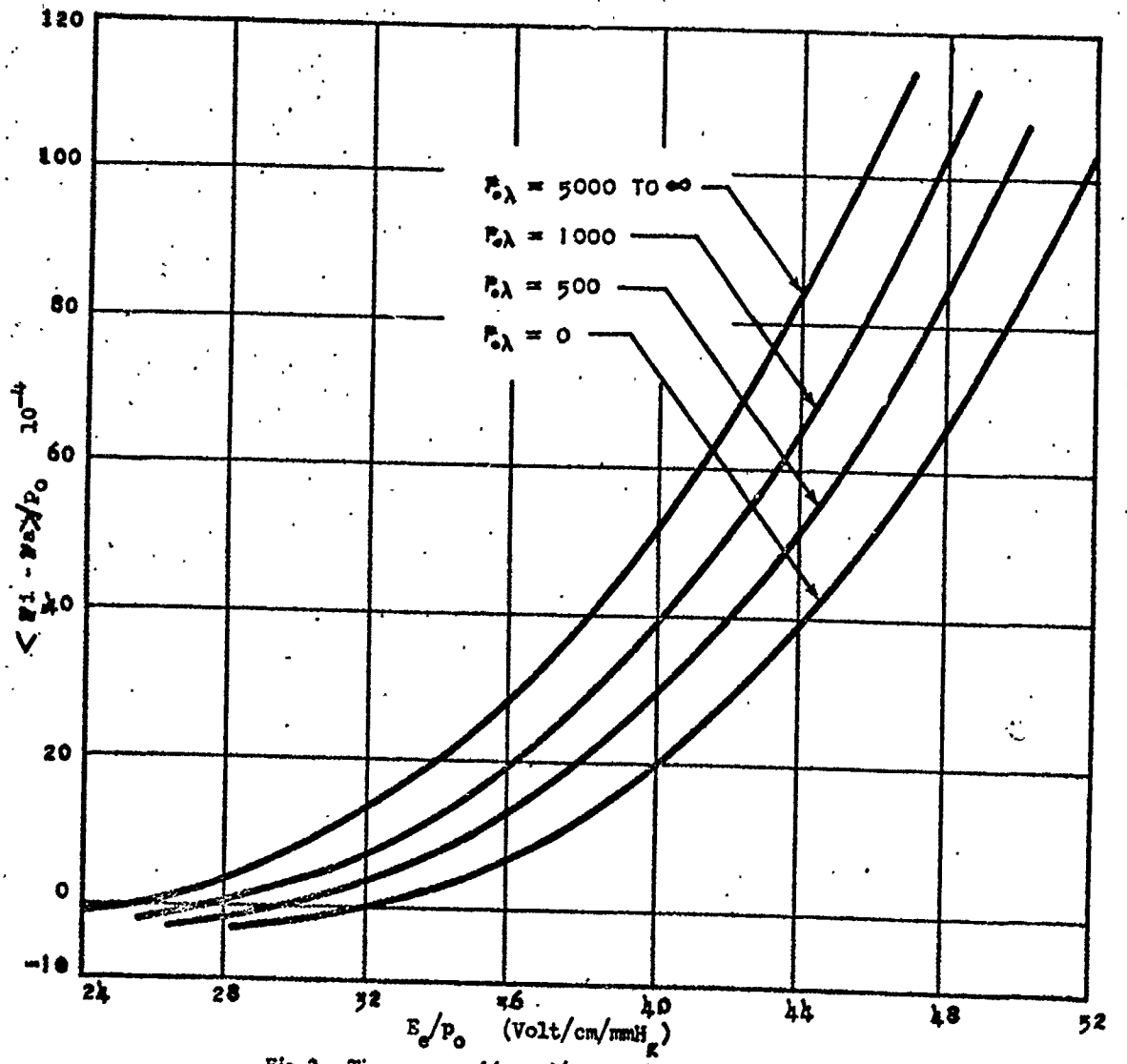

Fig. 2 Time average of $(\nu_i - \nu_a)/p_o$ as a function of E_e/p_o.

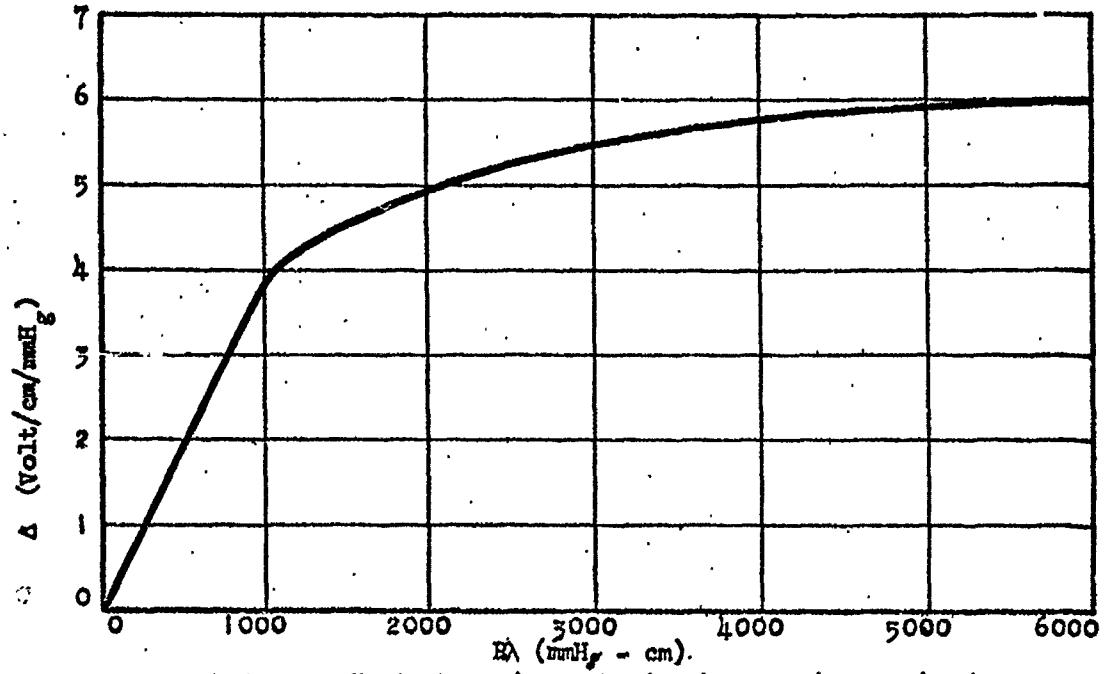

Fig. 3 Normalization factor, Δ, as a function of pressure times wavelength.

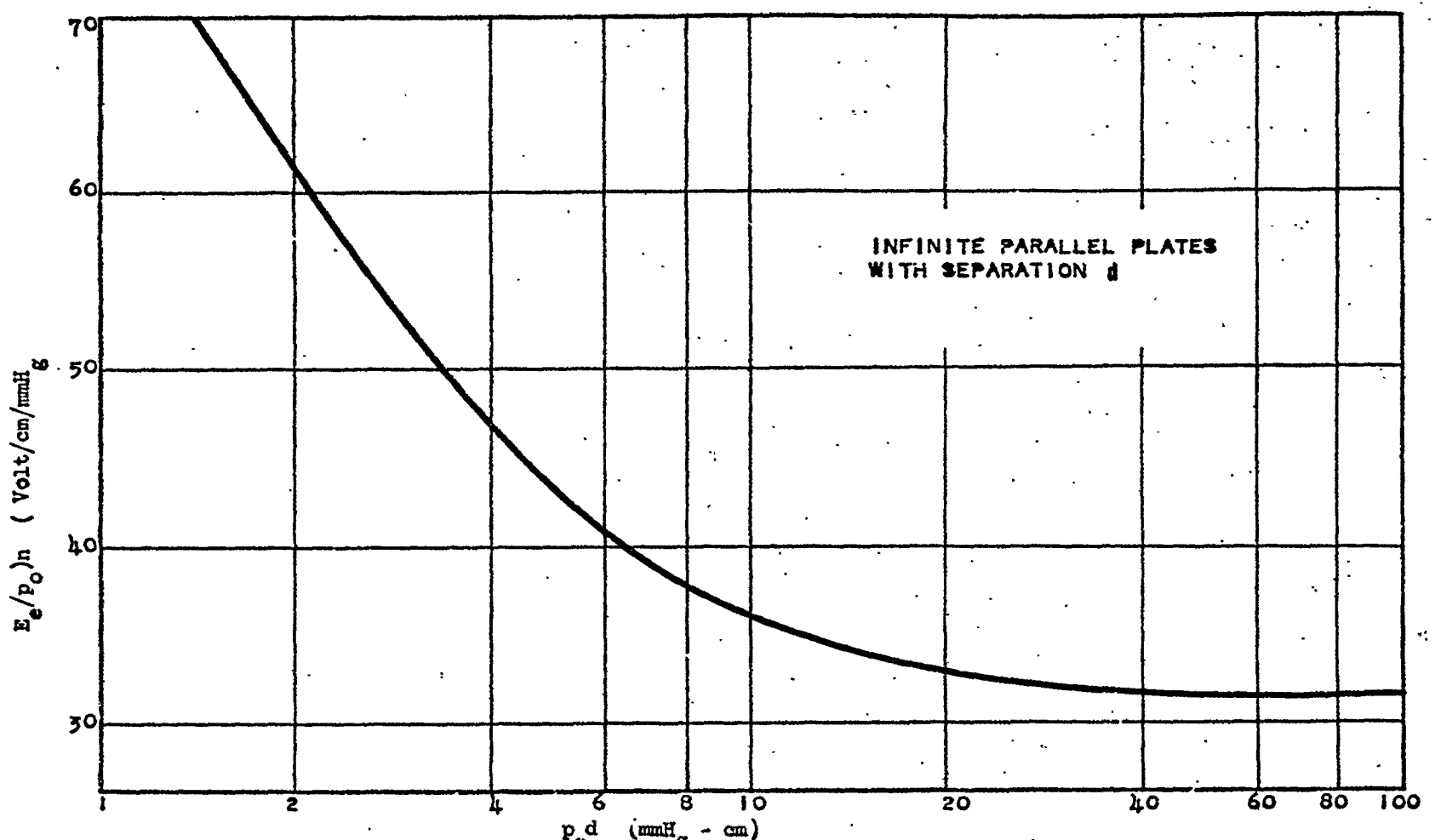

Fig. 4 Ratio of normalized cw breakdown field to pressure as a function of pressure times gap distance for infinite parallel plate geometry.

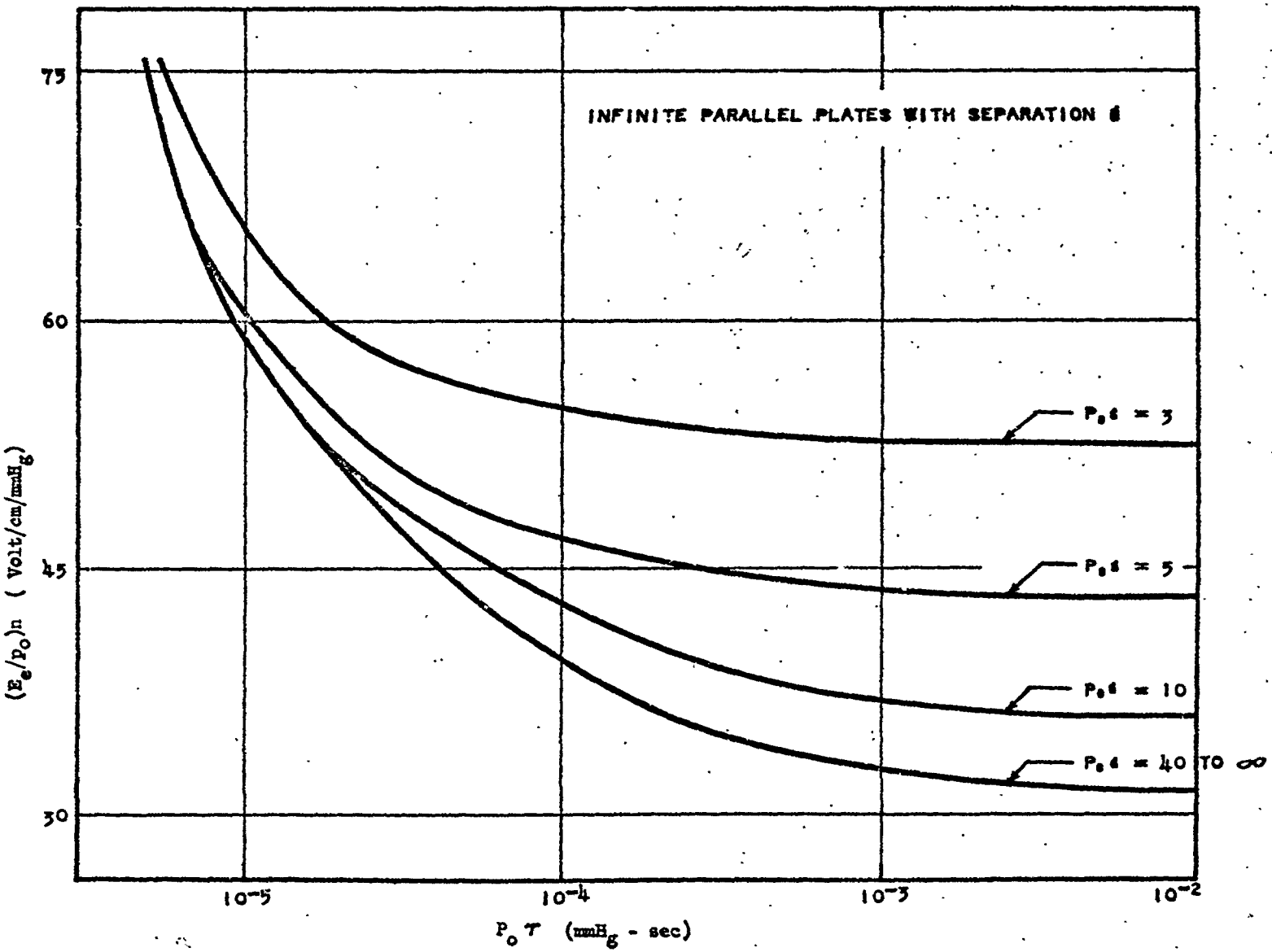

Fig. 5 Ratio of normalized single pulse effective breakdown field to pressure as a function of pressure times pulse width for various values of pressure times gap distance.

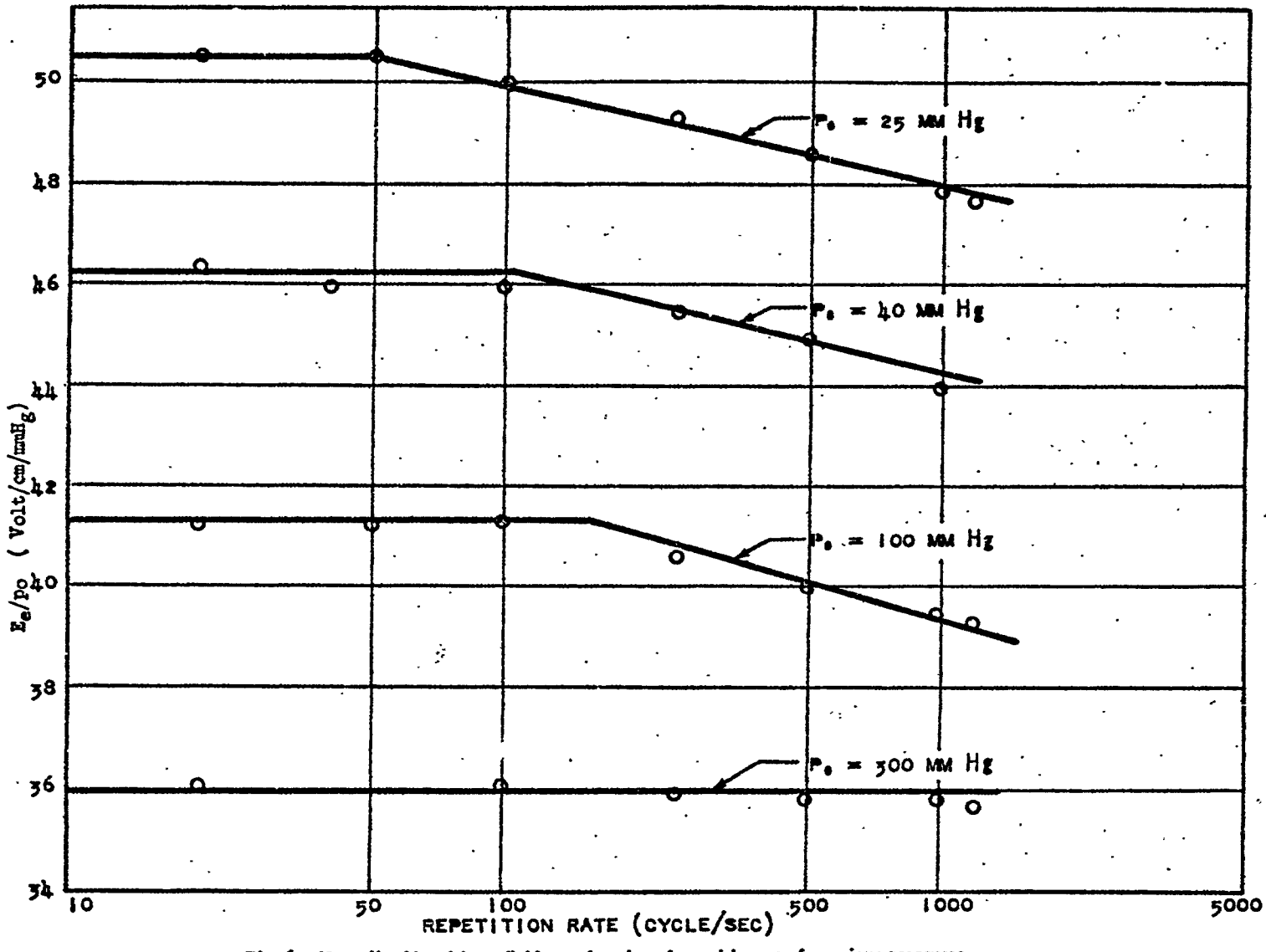

Fig. 6 Normalized breakdown field as a function of repetition rate for various pressures.

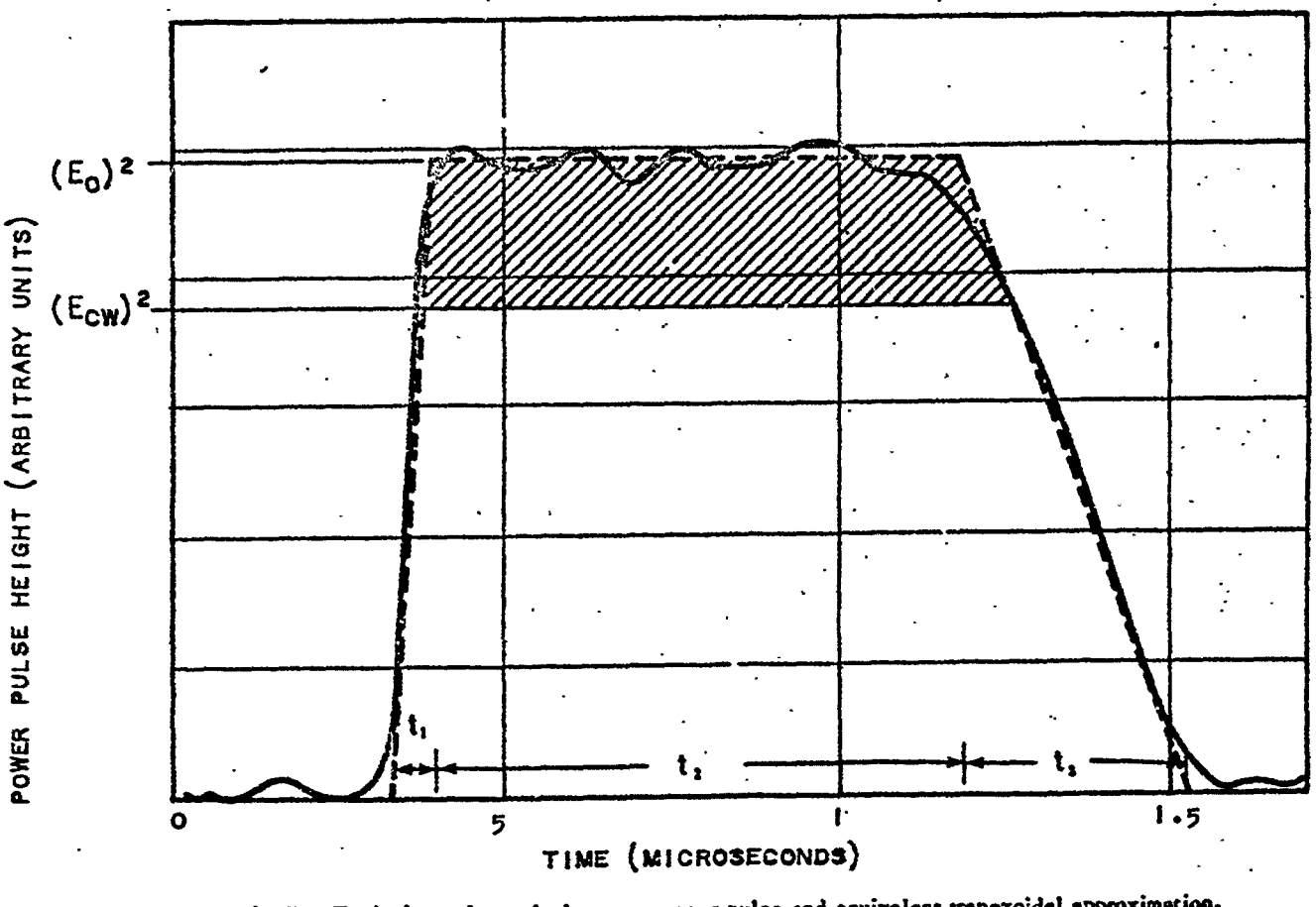

Fig. 7 Typical envelope of microwave power pulse and equivalent trapezoidal approximation.

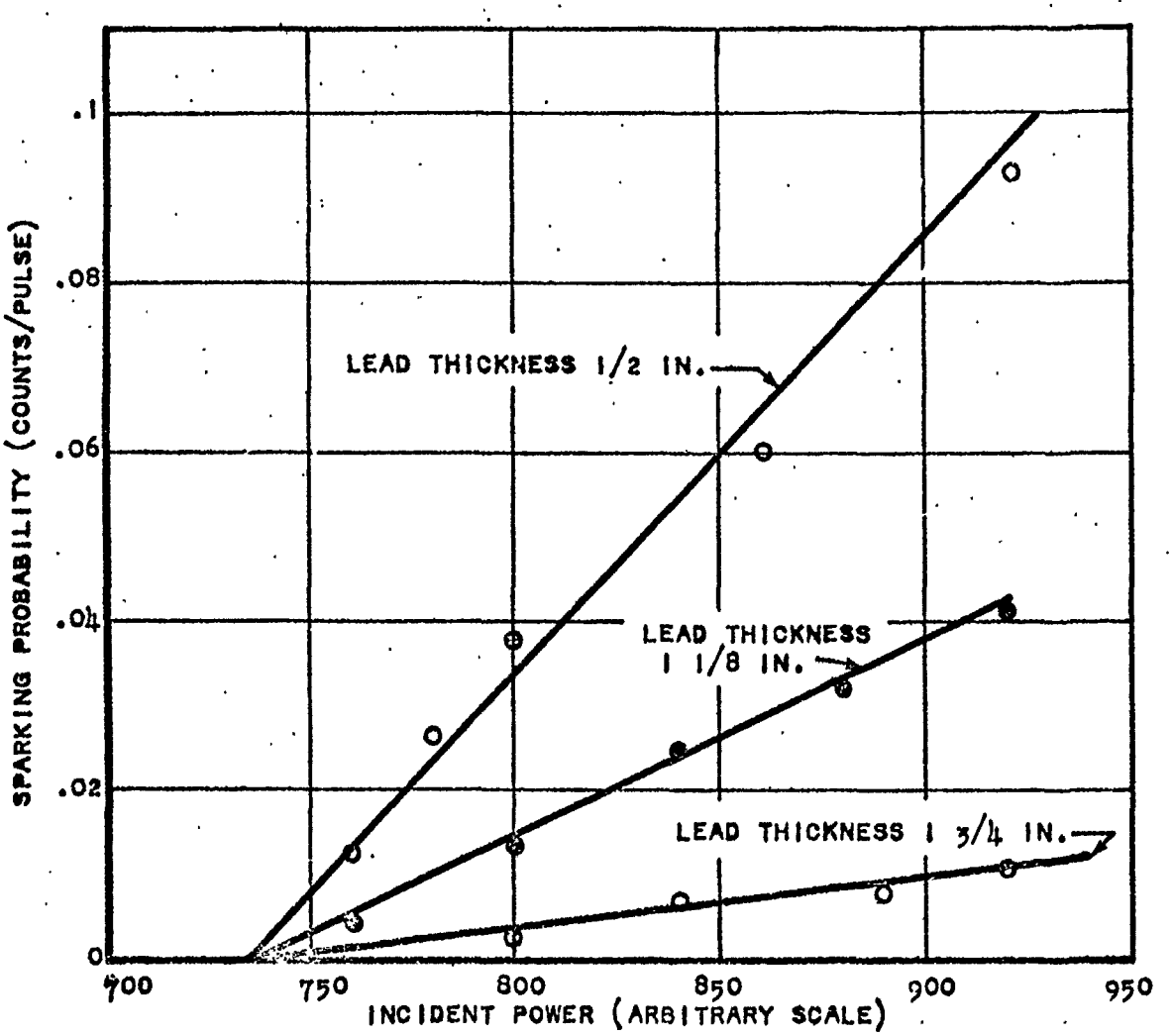

Fig. 8 Sparking probability as a function of incident power.

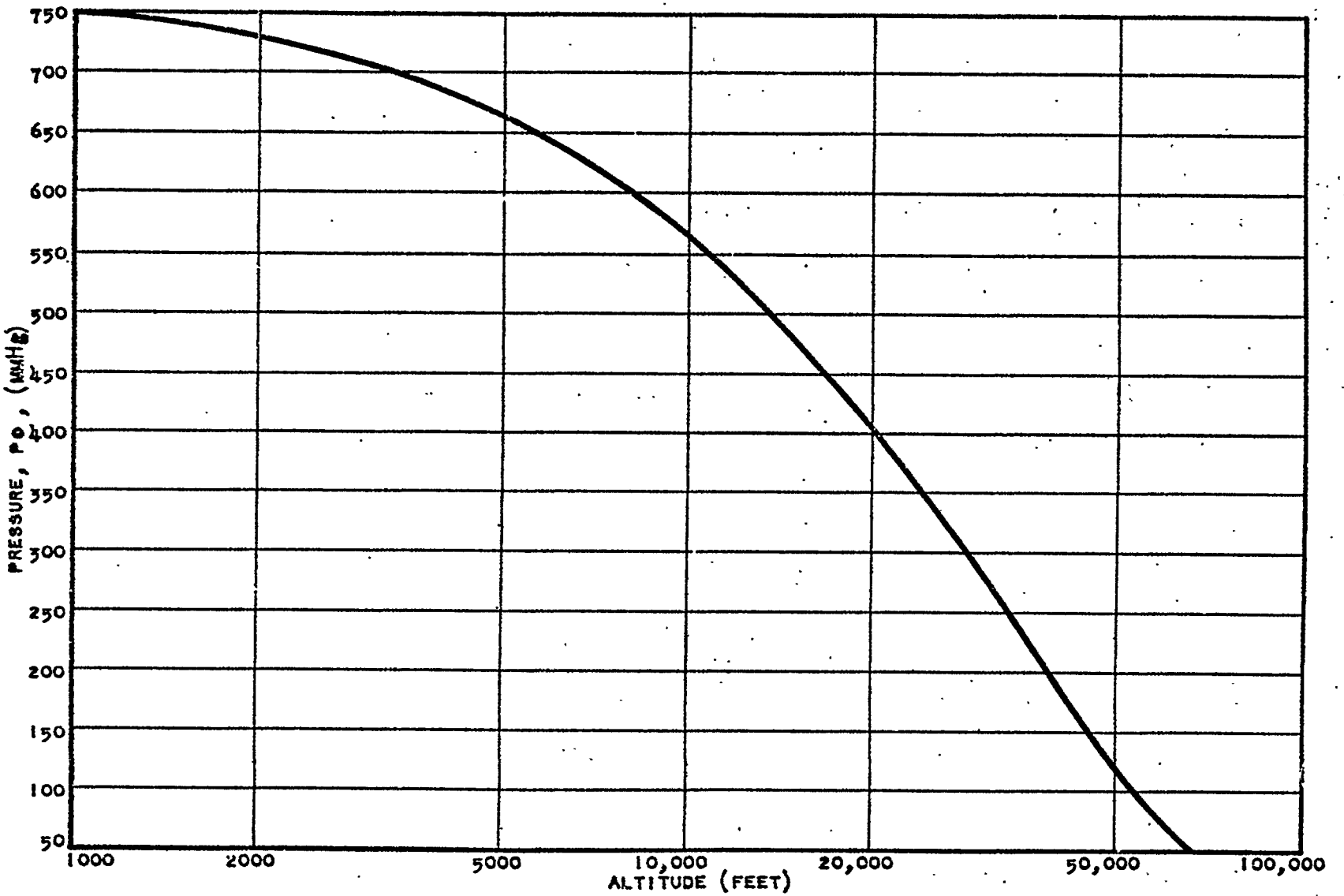

Fig. 9 Pressure, normalized to 20°C, as a function of altitude.

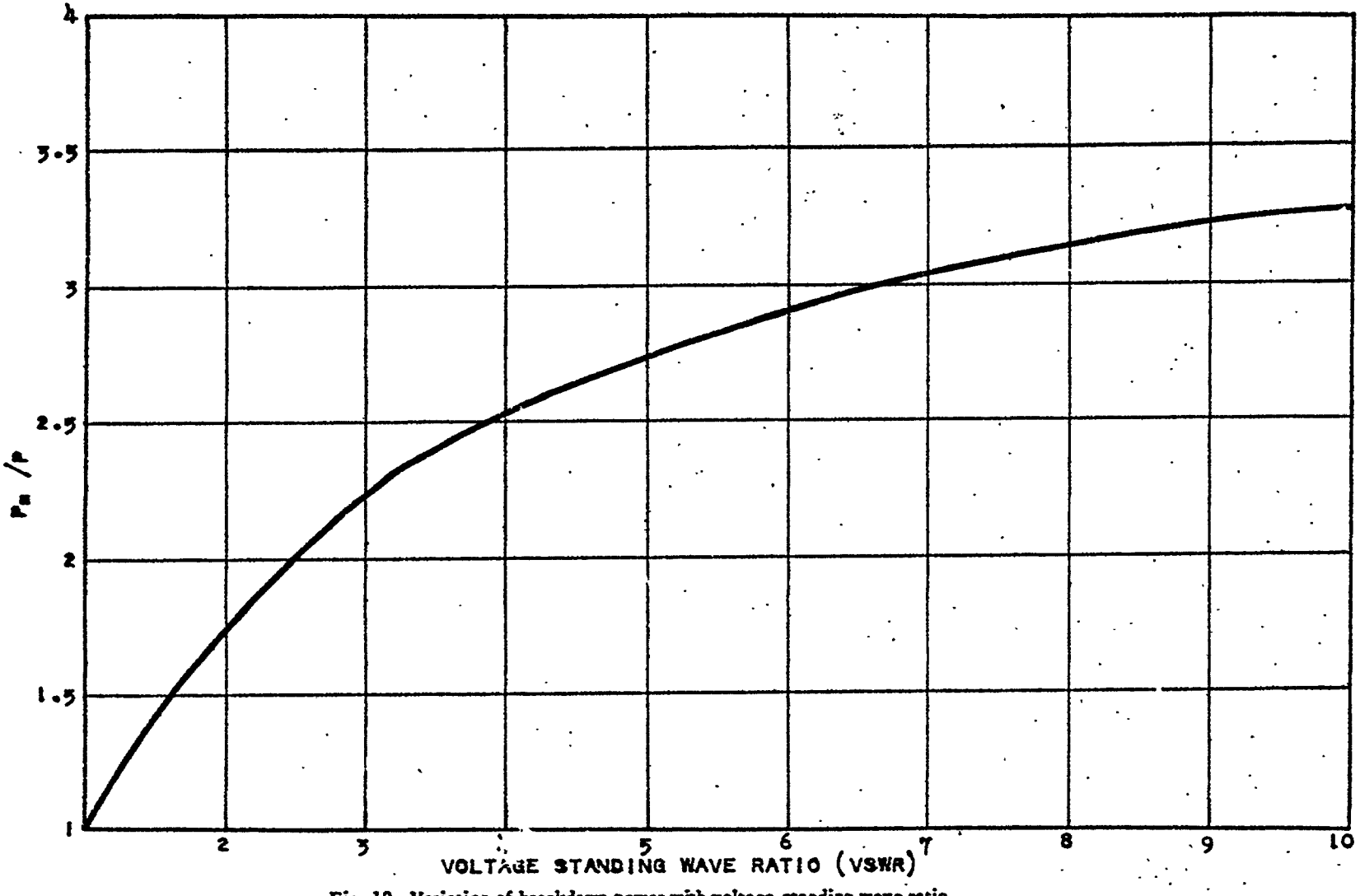

Fig. 10 Variation of breakdown power with voltage standing wave ratio.

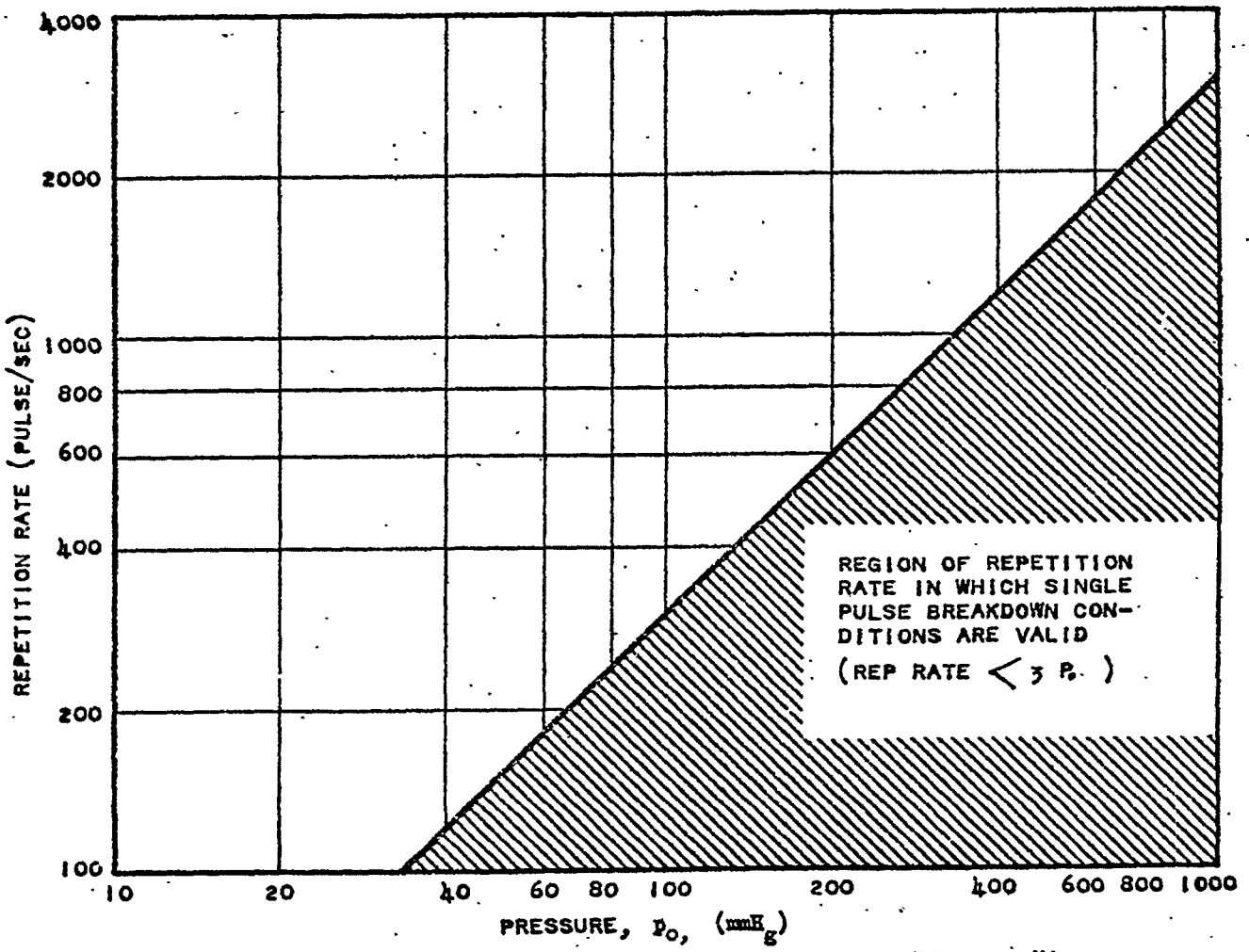

Fig. 11 Region of repetition rate in which single pulse breakdown conditions are valid.

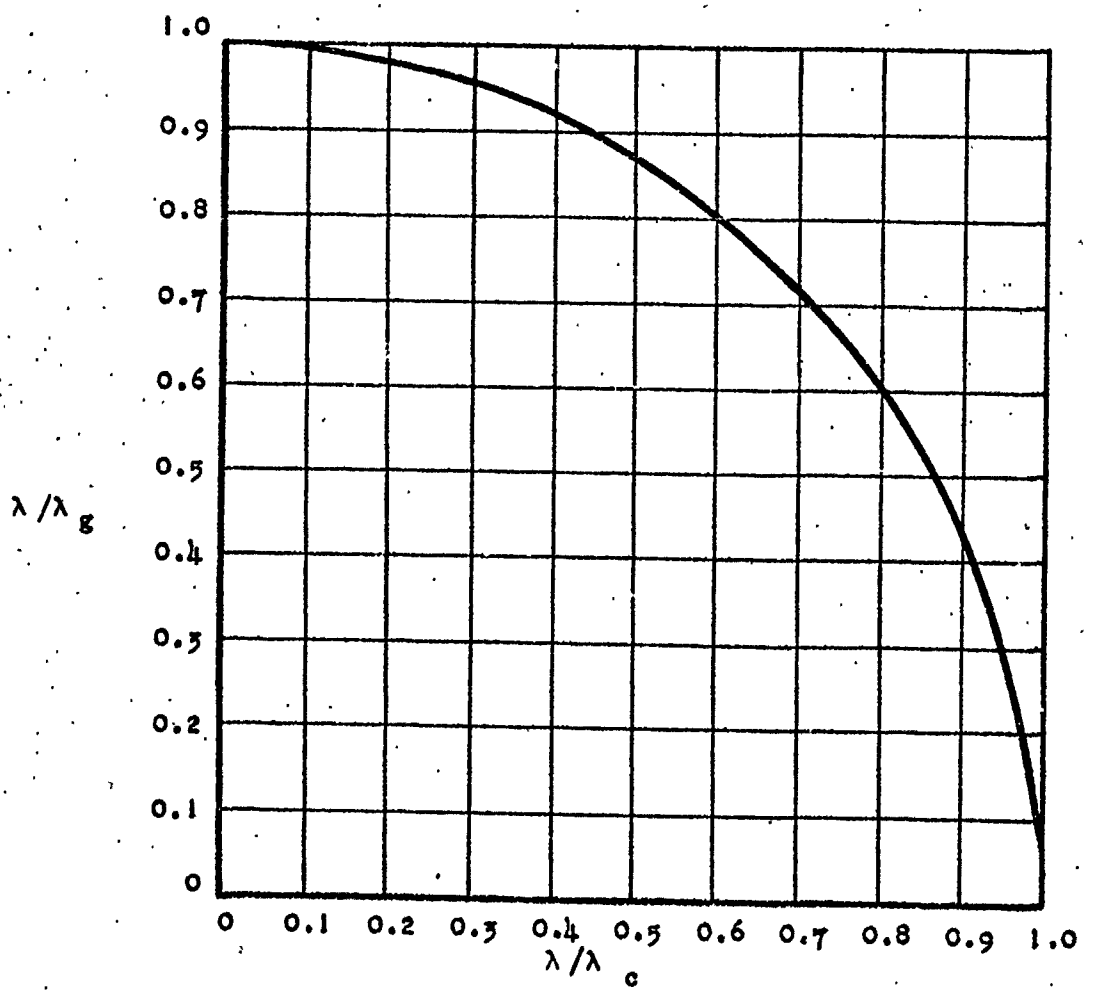

Fig. 12 λ/λ_g as a function of λ/λ_c.

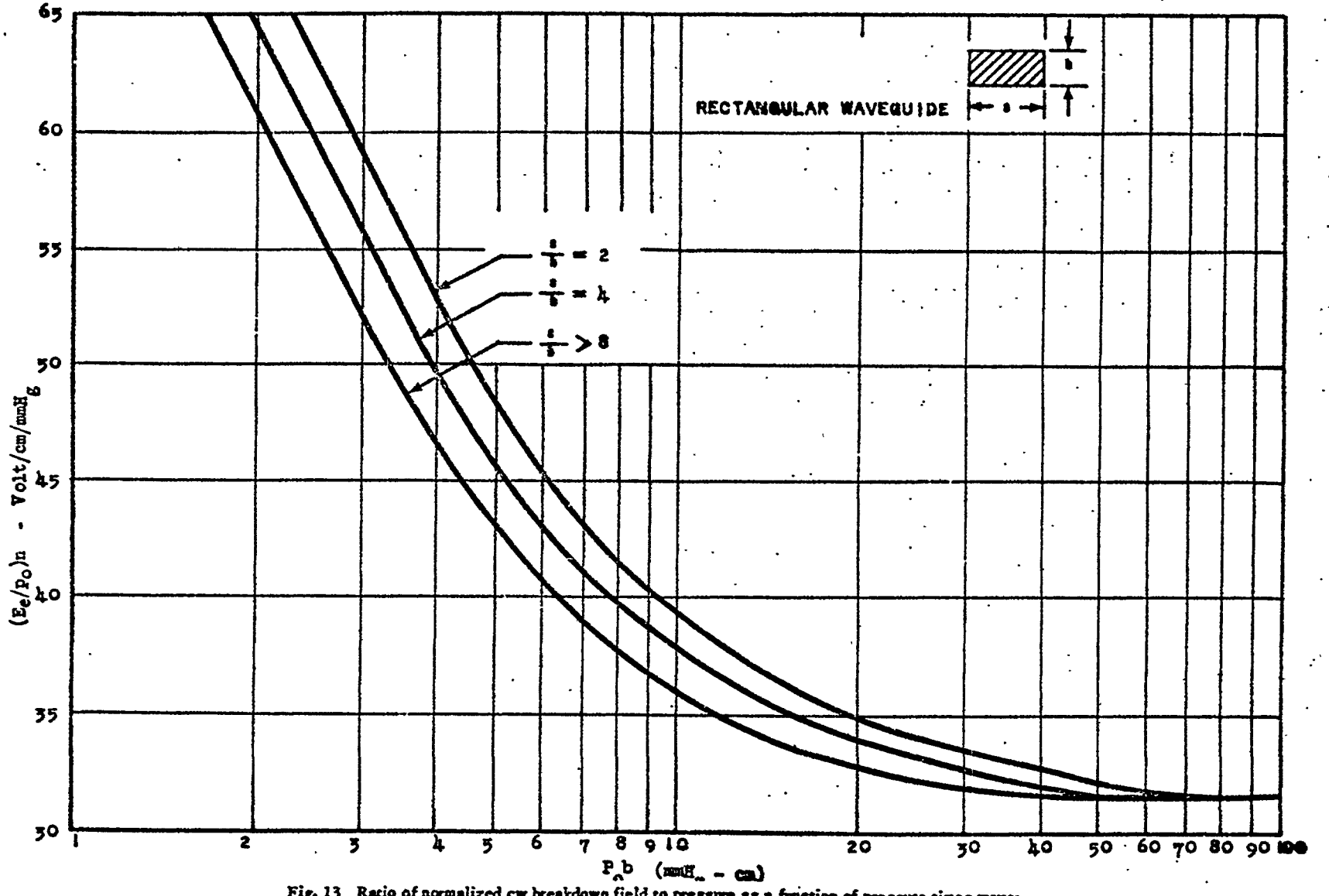

Fig. 13 Ratio of normalized cw breakdown field to pressure as a function of pressure times waveguide height for rectangular waveguide.

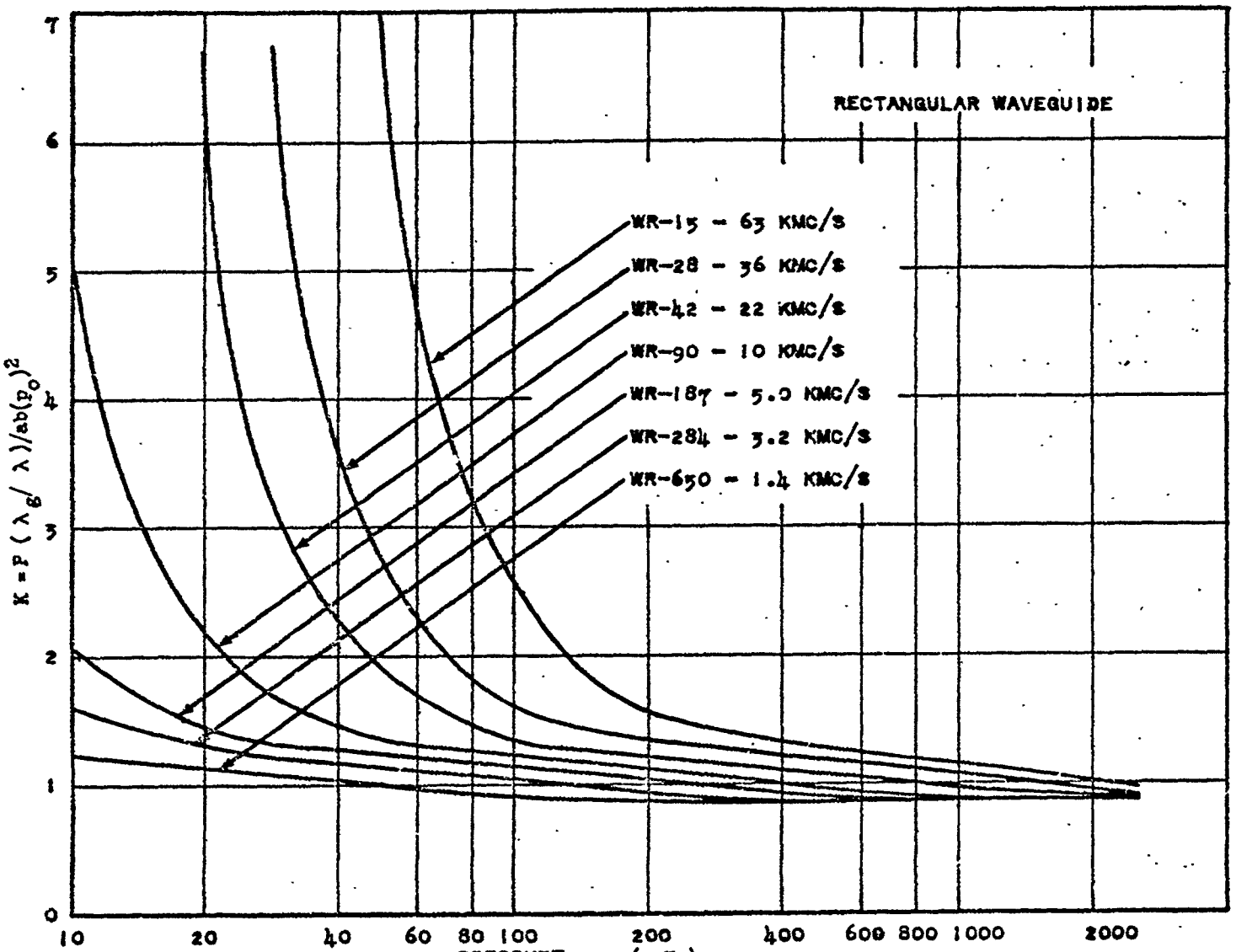

Fig. 14 CW breakdown power in terms of $P(\lambda_g/\lambda)/ab(p_o)^2$ as a function of pressure for rectangular waveguides.

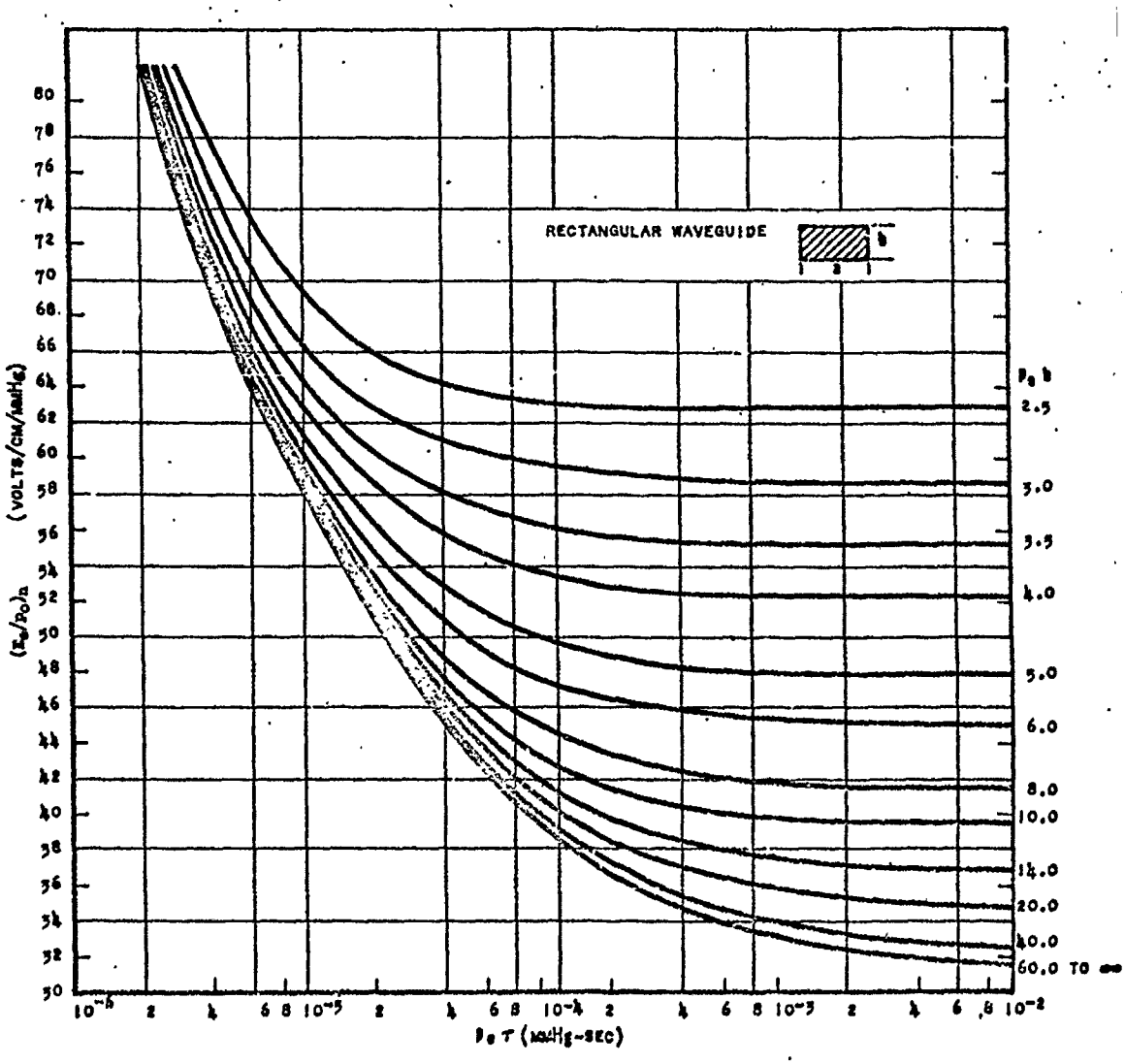

Fig. 15 Ratio of normalized single pulse breakdown field to pressure as a function of pressure times pulse width for various values of pressure times waveguide height and for a/b=2.

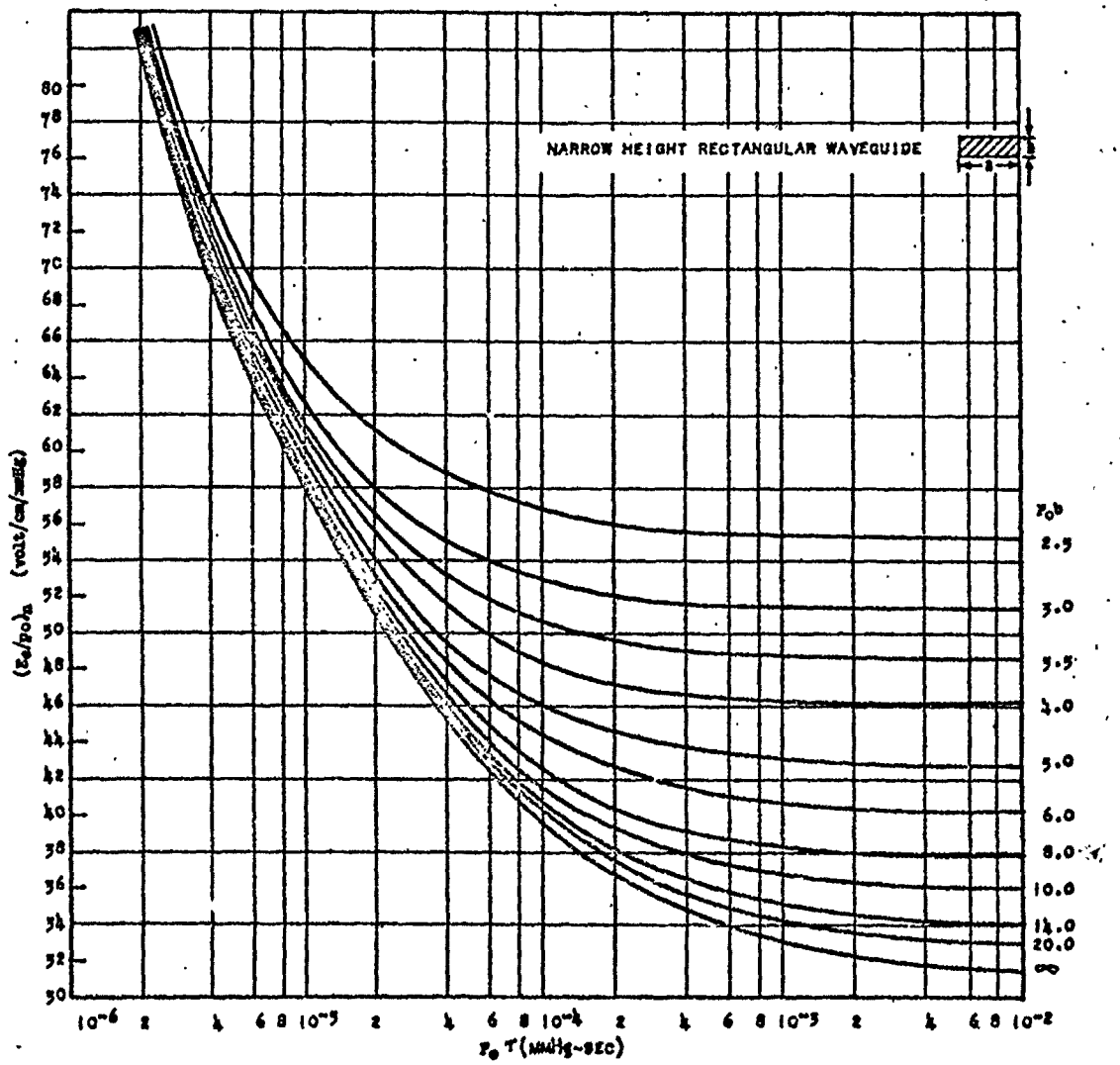

Fig. 16 Ratio of normalized single pulse breakdown field to pressure as a function of pressure times pulse width for various values of pressure times waveguide height and for $a/b > 2$.

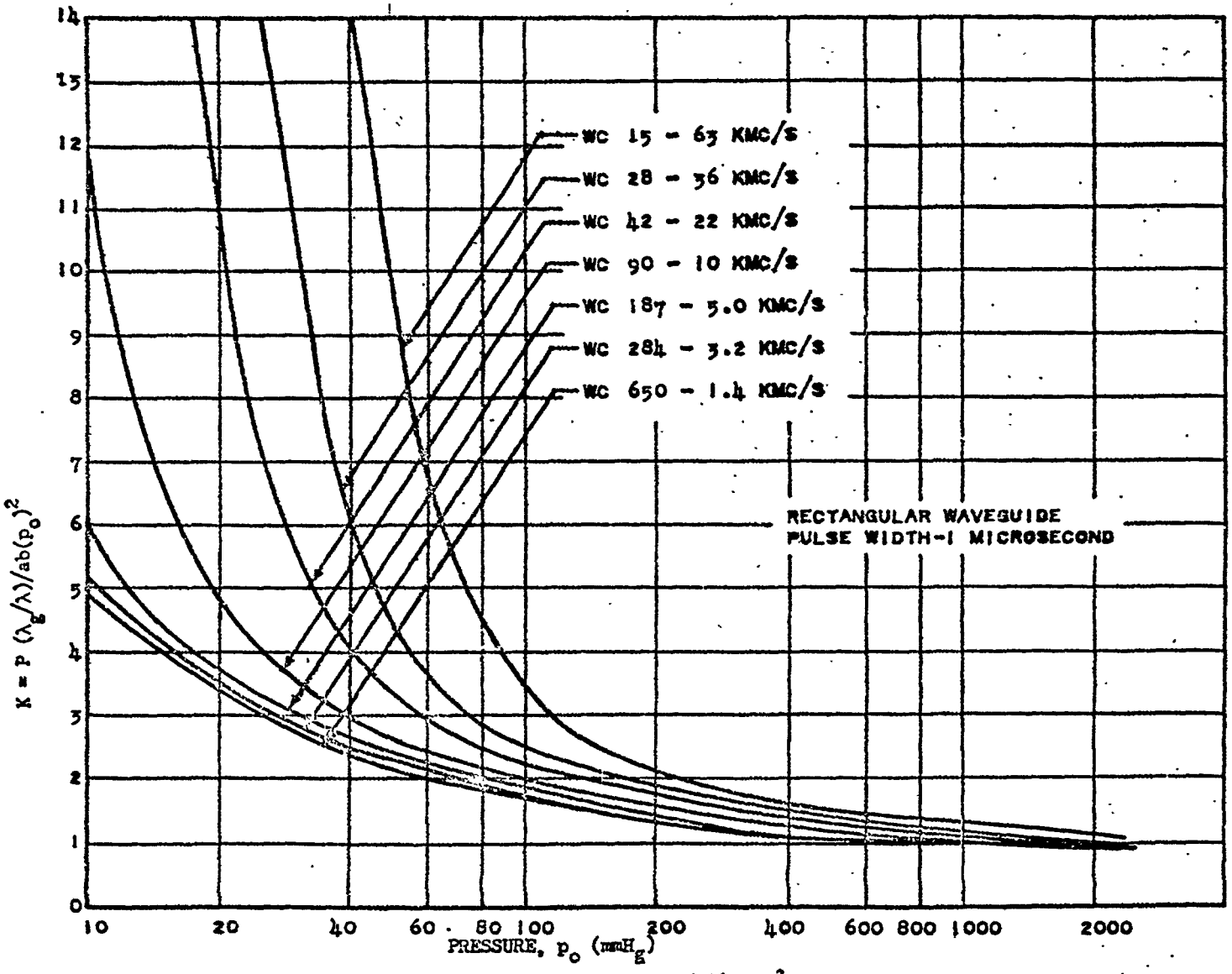

Fig. 17 Single pulse breakdown power in terms of $P(\lambda_g/\lambda)/ab(p_o)^2$ as a function of pressure for rectangular waveguides and for a one microsecond pulse.

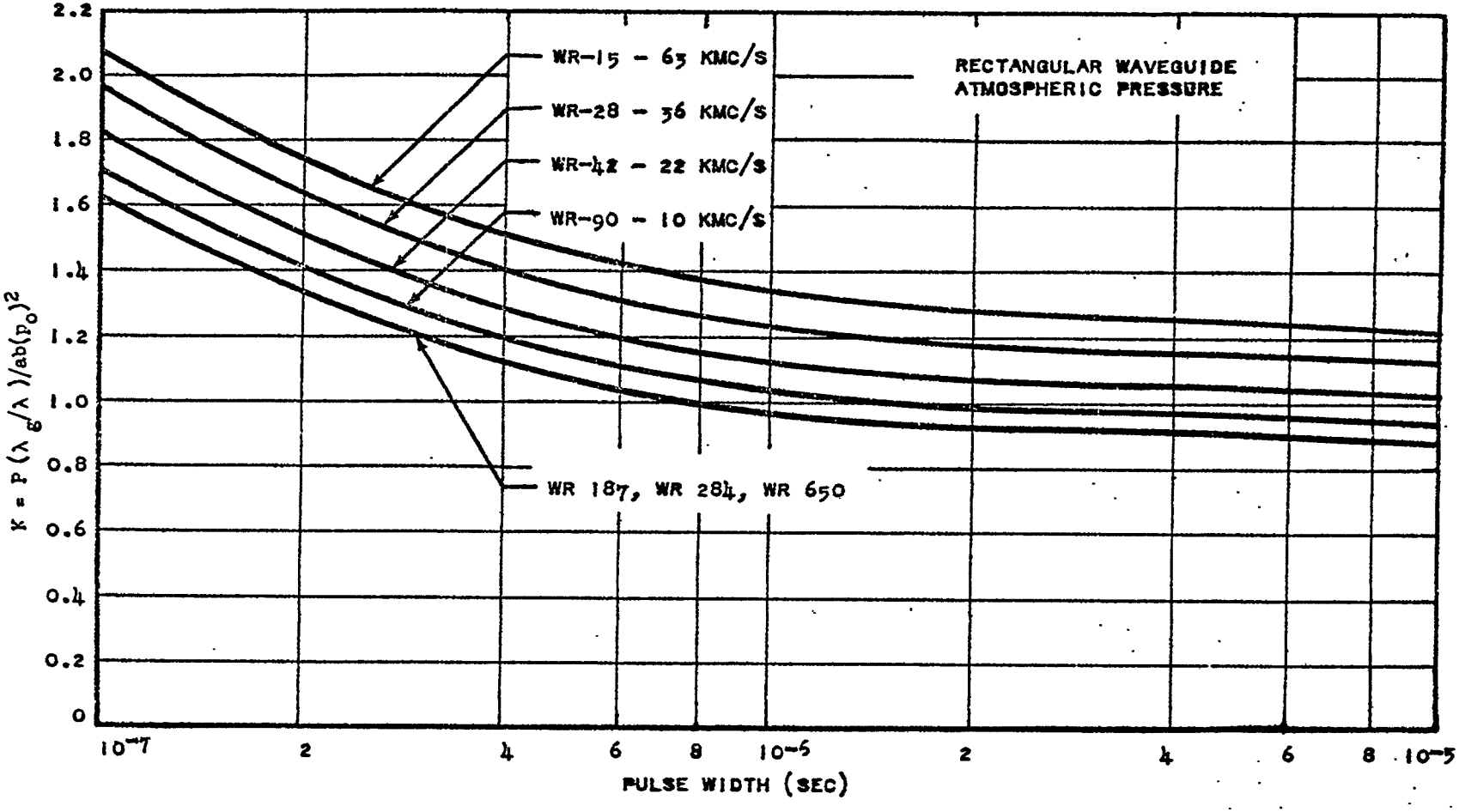

Fig. 18 Single pulse breakdown power in terms of $P(\lambda_g/\lambda)/ab(p_o)^2$ as a function of pulse width at atmospheric pressure (760 mm Hg) for rectangular waveguides.

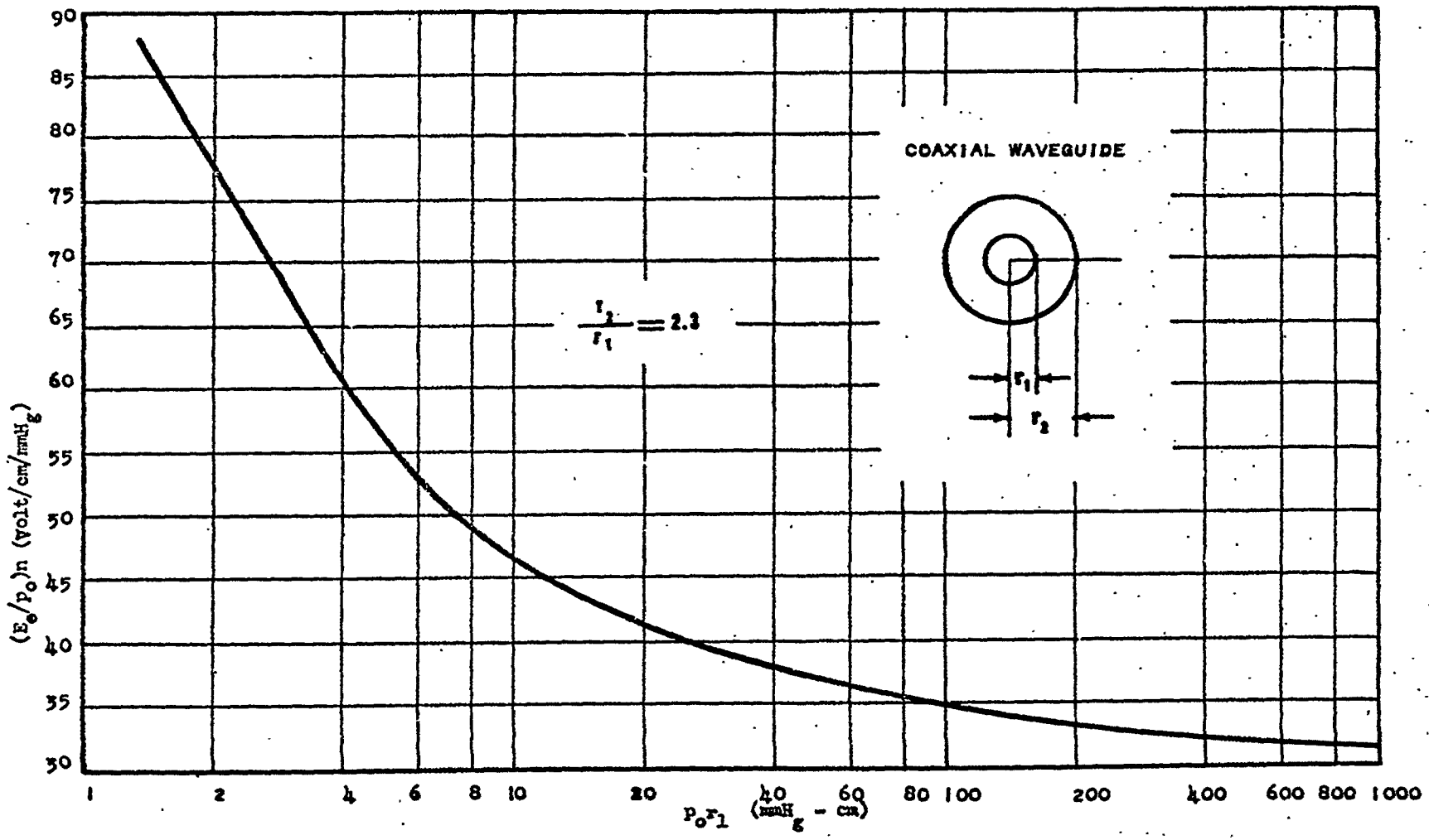

Fig. 19 Ratio of normalized cw breakdown field to pressure as a function of pressure times inner conductor radius.

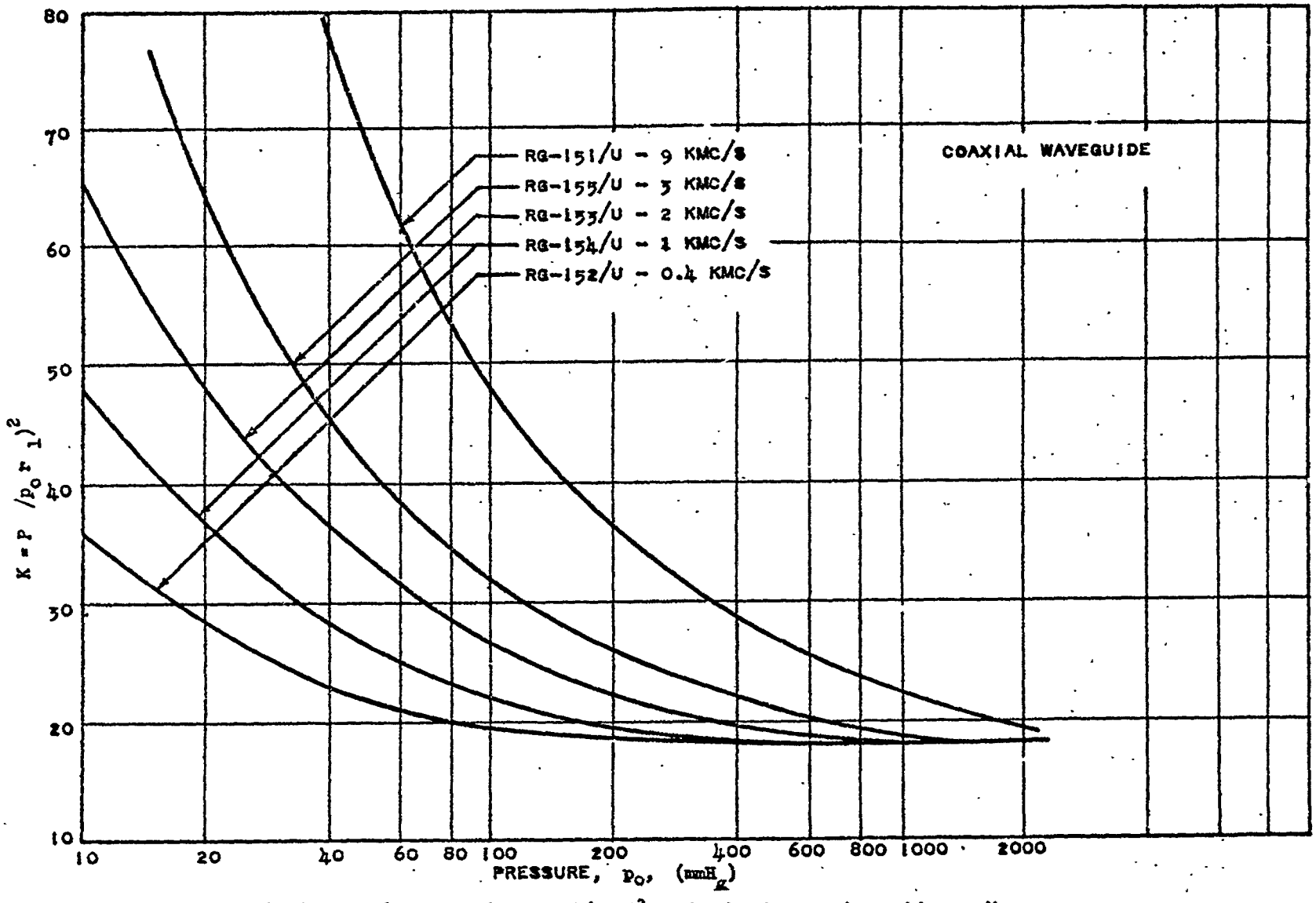

Fig. 20 CW breakdown power in terms of $P/(p_g r_1)^2$ as a function of pressure for coaxial waveguides.

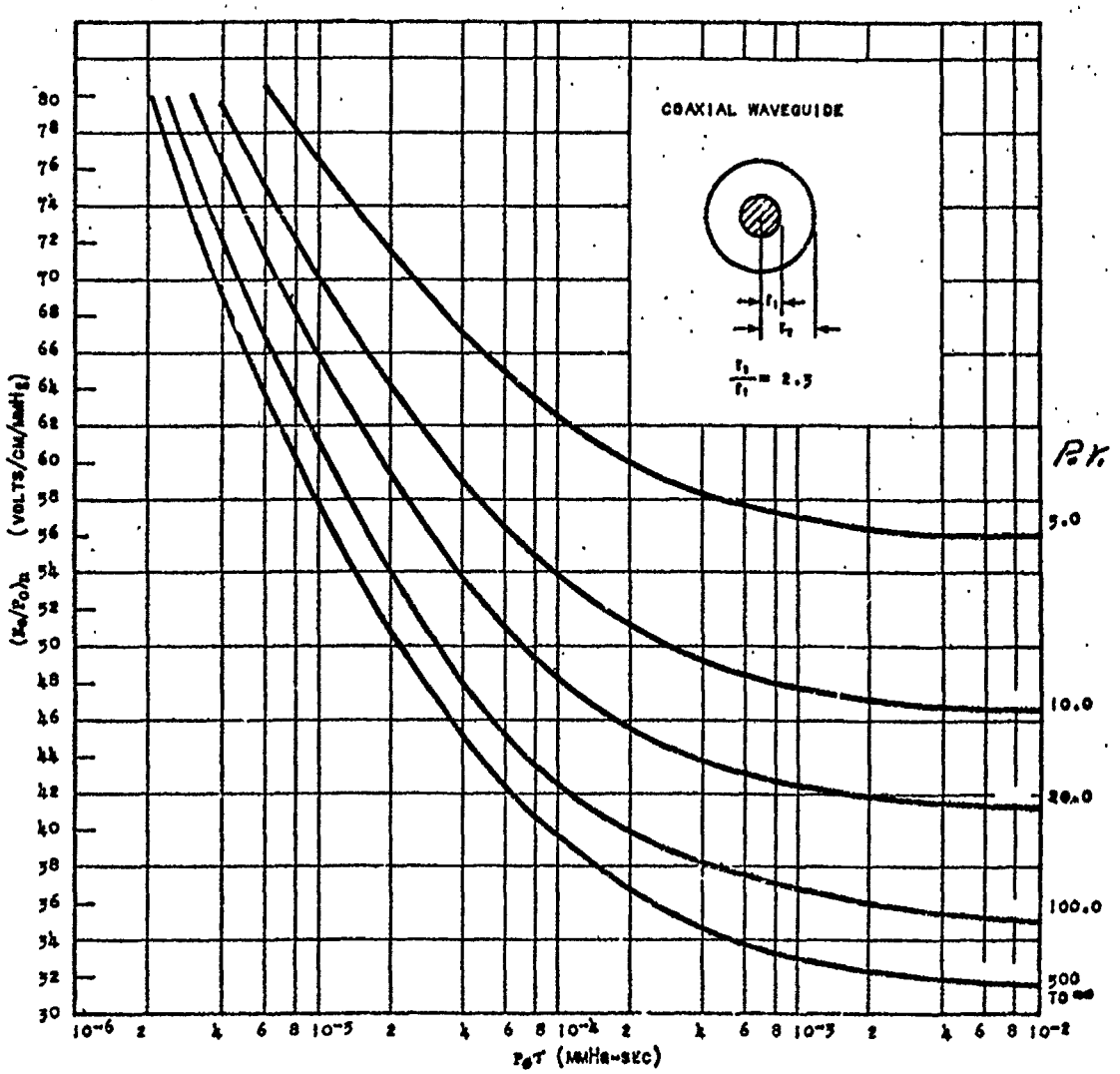

Fig. 21 Ratio of normalized single pulse breakdown field to pressure as a function of pressure times pulse width for various values of pressure times inner conductor radius.

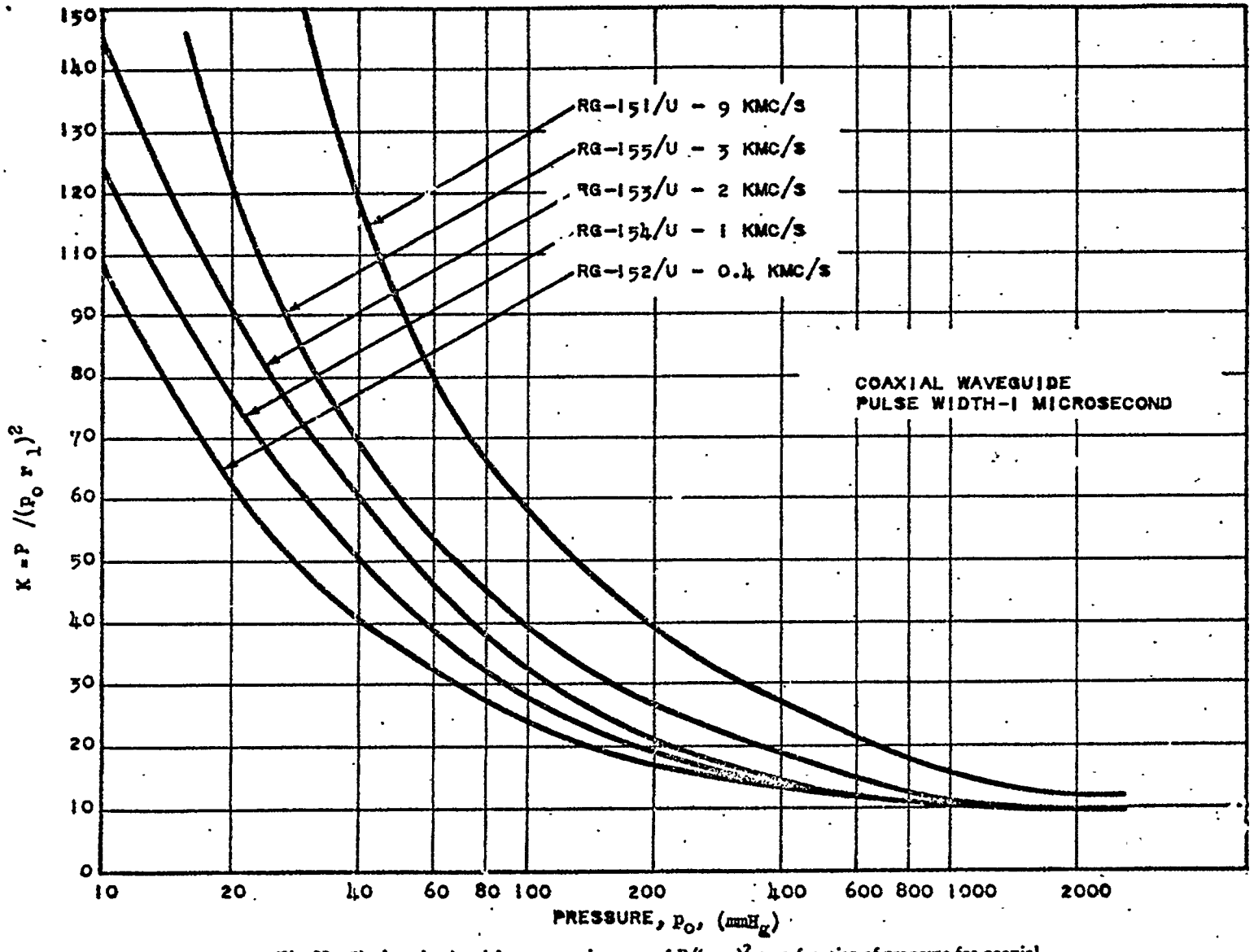

Fig. 22 Single pulse breakdown power in terms of $P/(p_o r_1)^2$ as a function of pressure for coaxial waveguides and for a one microsecond pulse.

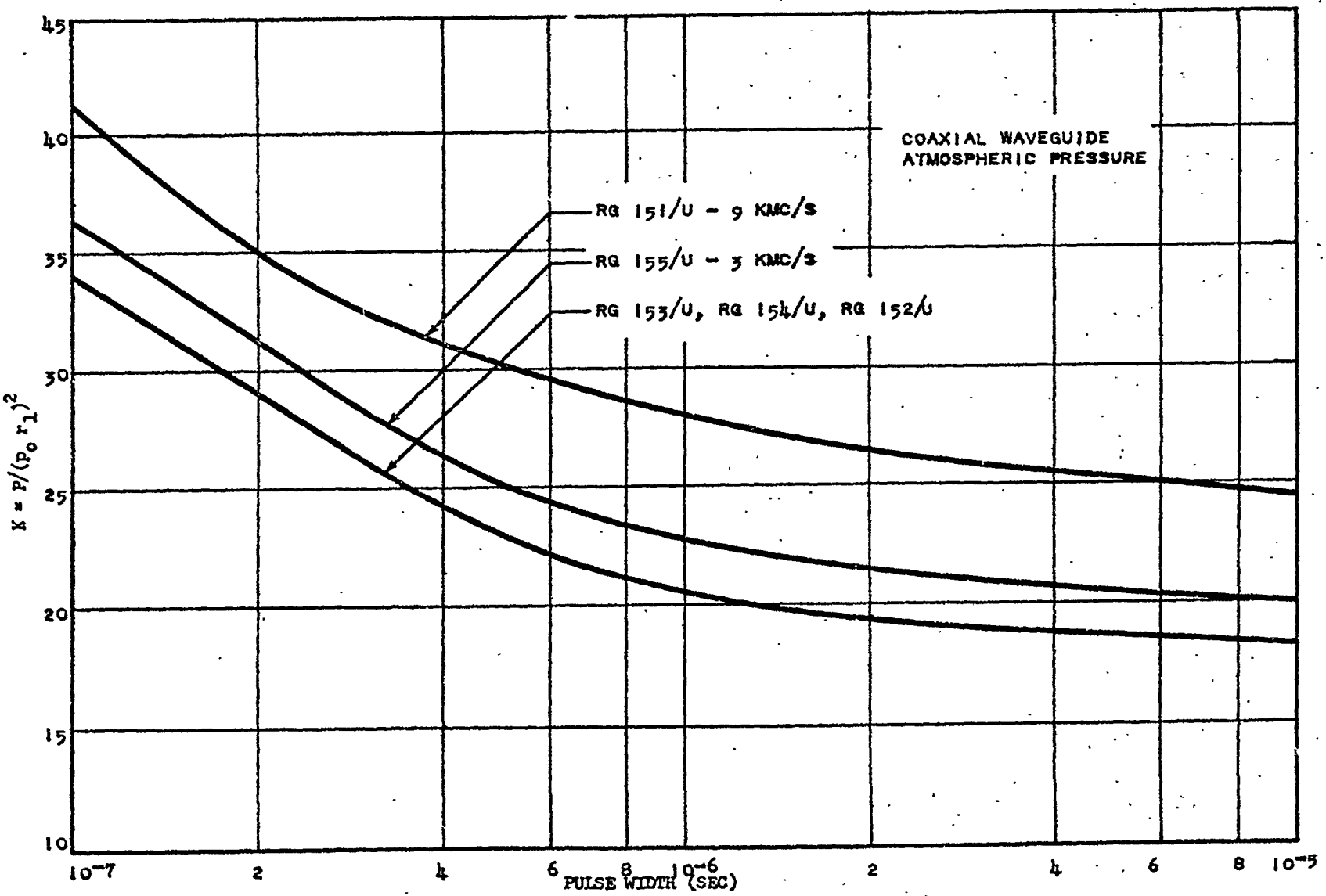

Fig. 23 Single pulse breakdown power in terms of $P/(p_o r_1)^2$ as a function of pulse width for coaxial waveguides.

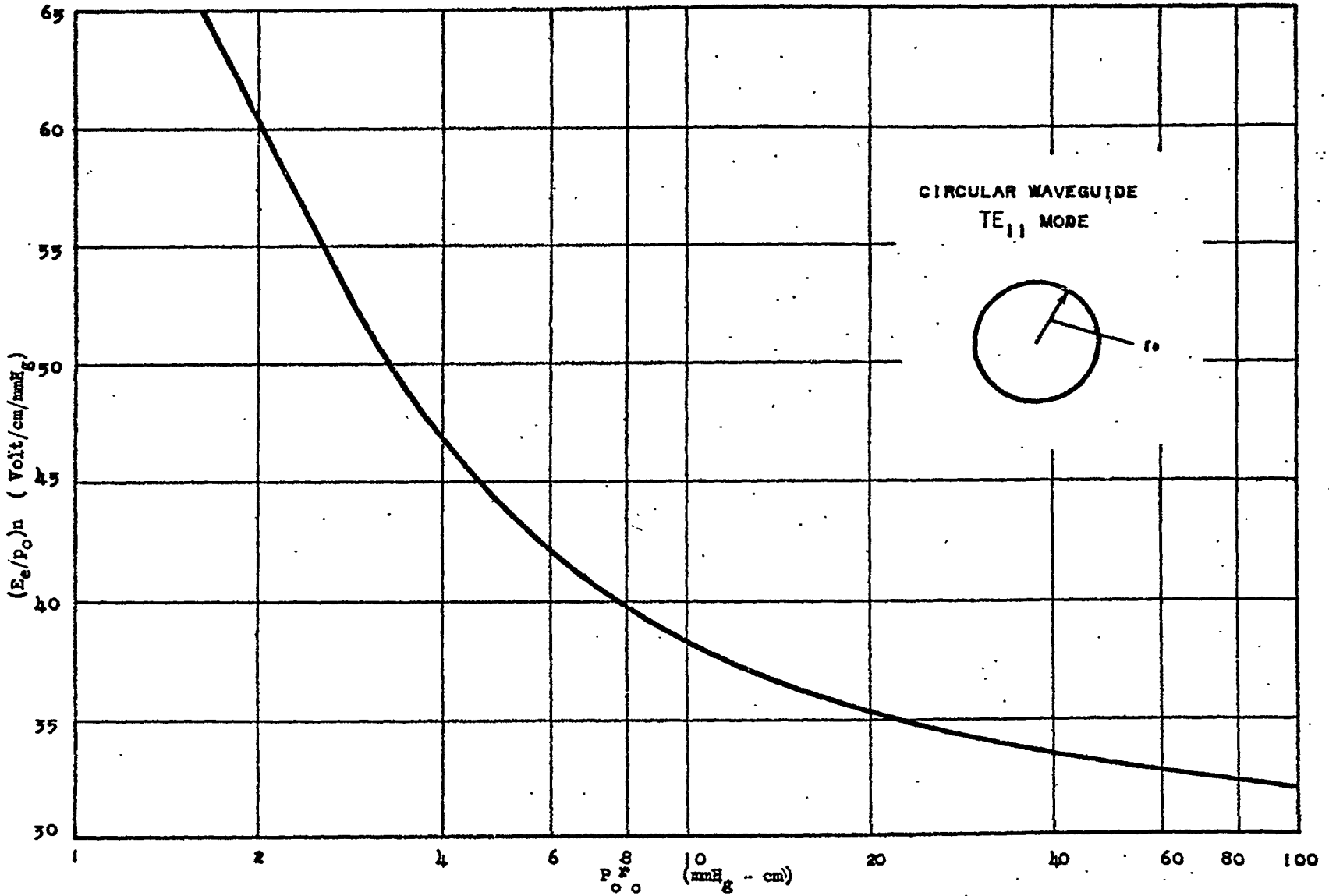

Fig. 24 Ratio of normalized cw breakdown field to pressure as a function of pressure times radius for circular waveguide operating in the TE_{11} mode.

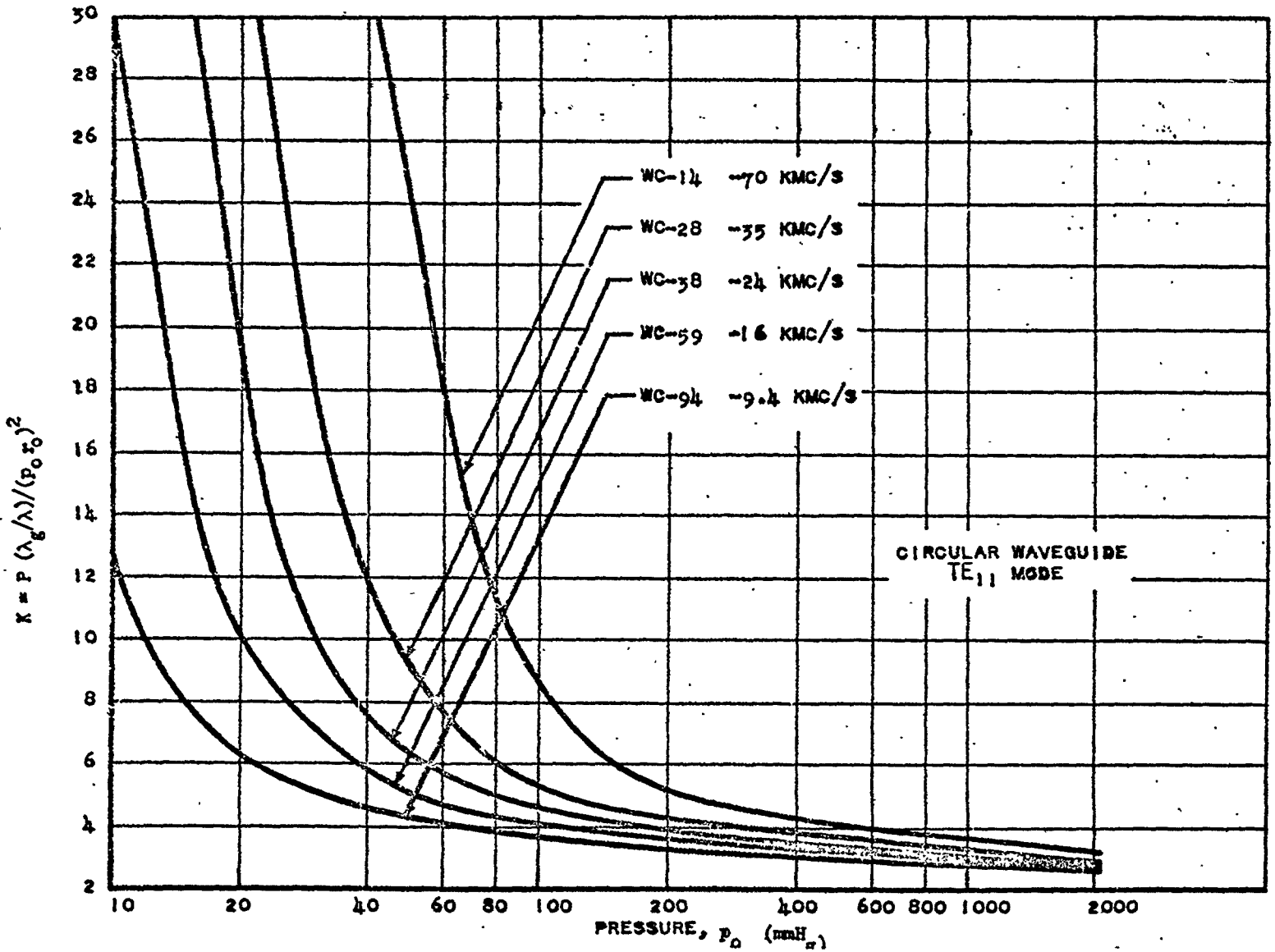

Fig. 25 CW breakdown power in terms of $P(\lambda_g/\lambda)/(p_0 r_0)^2$ as a function of pressure for circular waveguide operating in the TE_{11} mode.

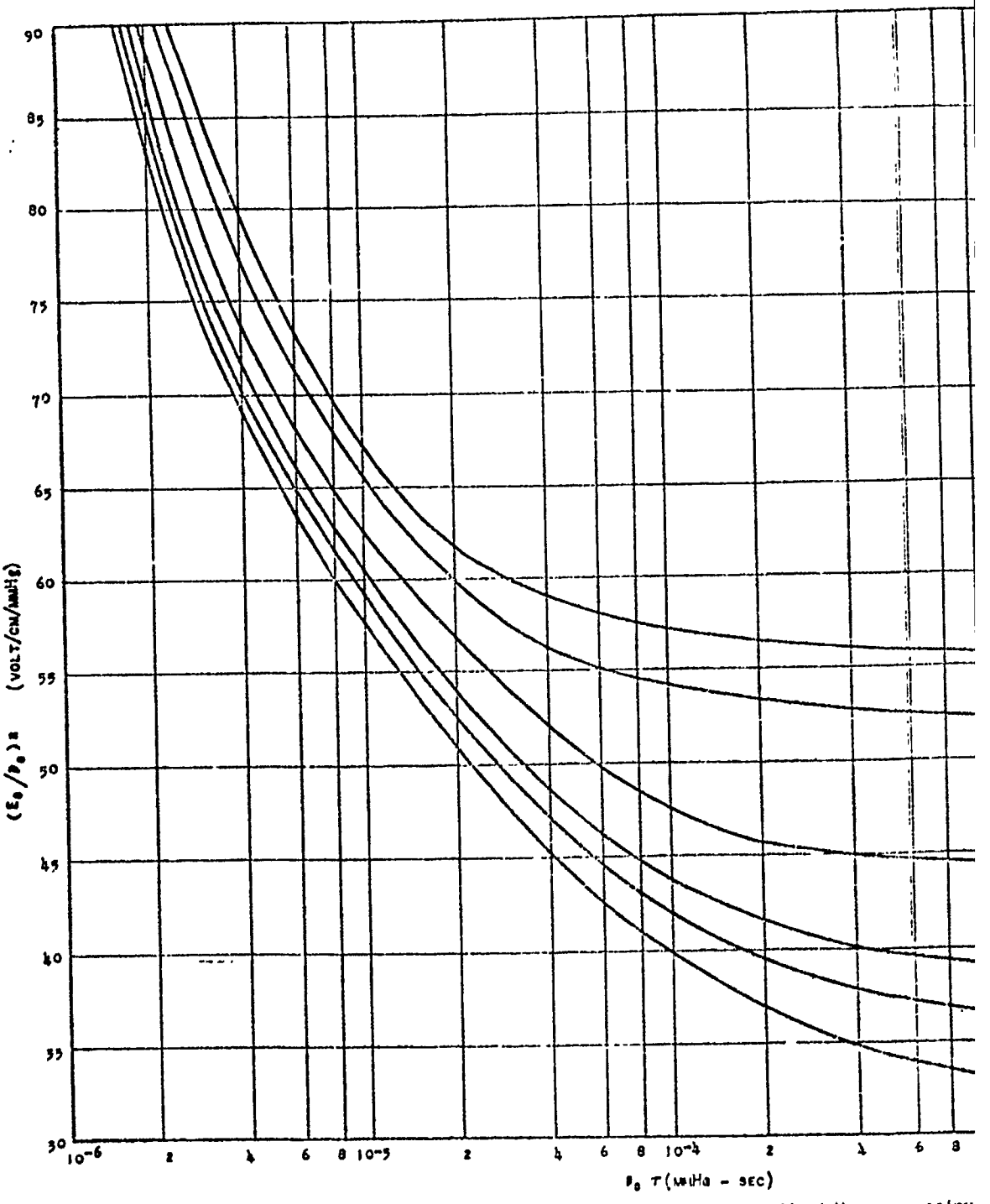

Fig. 26 Ratio of normalized single pulse breakdown field to pressure as a funct
times pulse width for various values of pressure times radius for circul
operating in the TE_{11} mode.

(1)

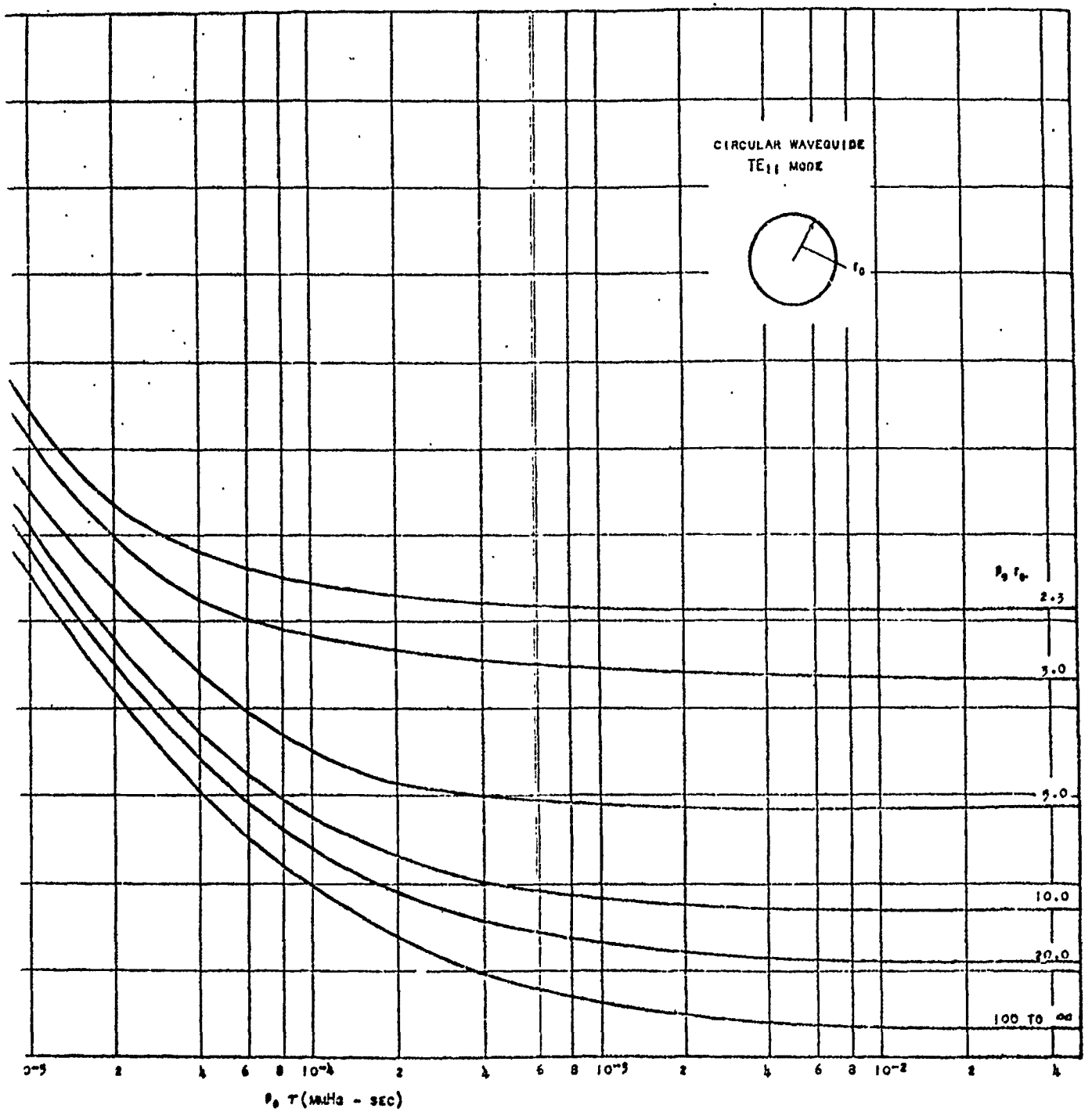

Fig. 26 Ratio of normalized single pulse breakdown field to pressure as a function of pressure times pulse width for various values of pressure times radius for circular waveguides operating in the TE_{11} mode.

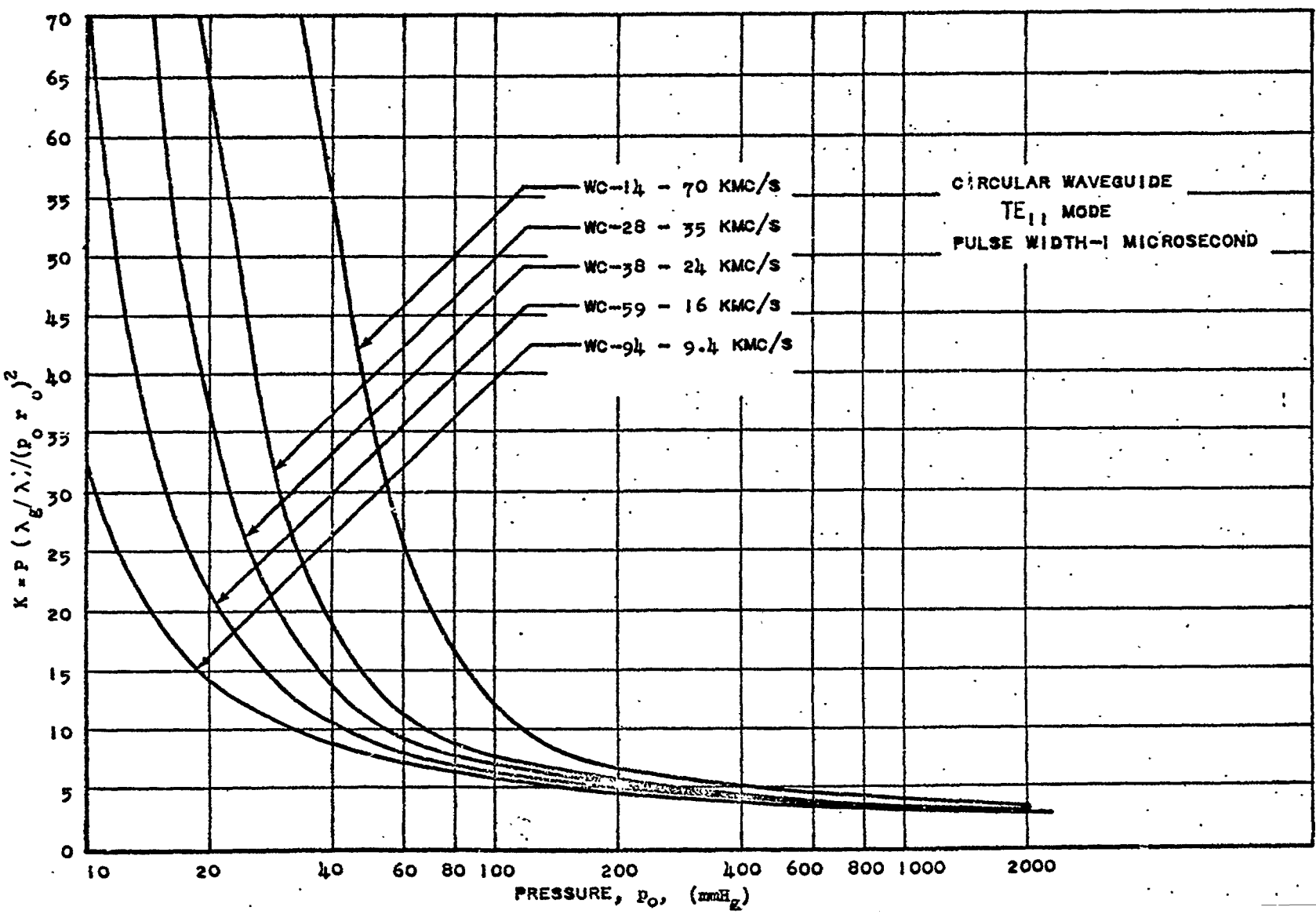
WC-14 - 70 KMC/S
WC-28 - 35 KMC/S
WC-38 - 24 KMC/S
WC-59 - 16 KMC/S
WC-94 - 9.4 KMC/S
CIRCULAR WAVEGUIDE
TE11 MODE
PULSE WIDTH-1 MICROSECOND
K = P (λg/λ)/(p0 r0)2
PRESSURE, p0, (mmHg)
0
5
10
15
20
25
30
35
40
45
50
55
60
65
70
10
20
40
60
80
100
200
400
600
800
1000
2000

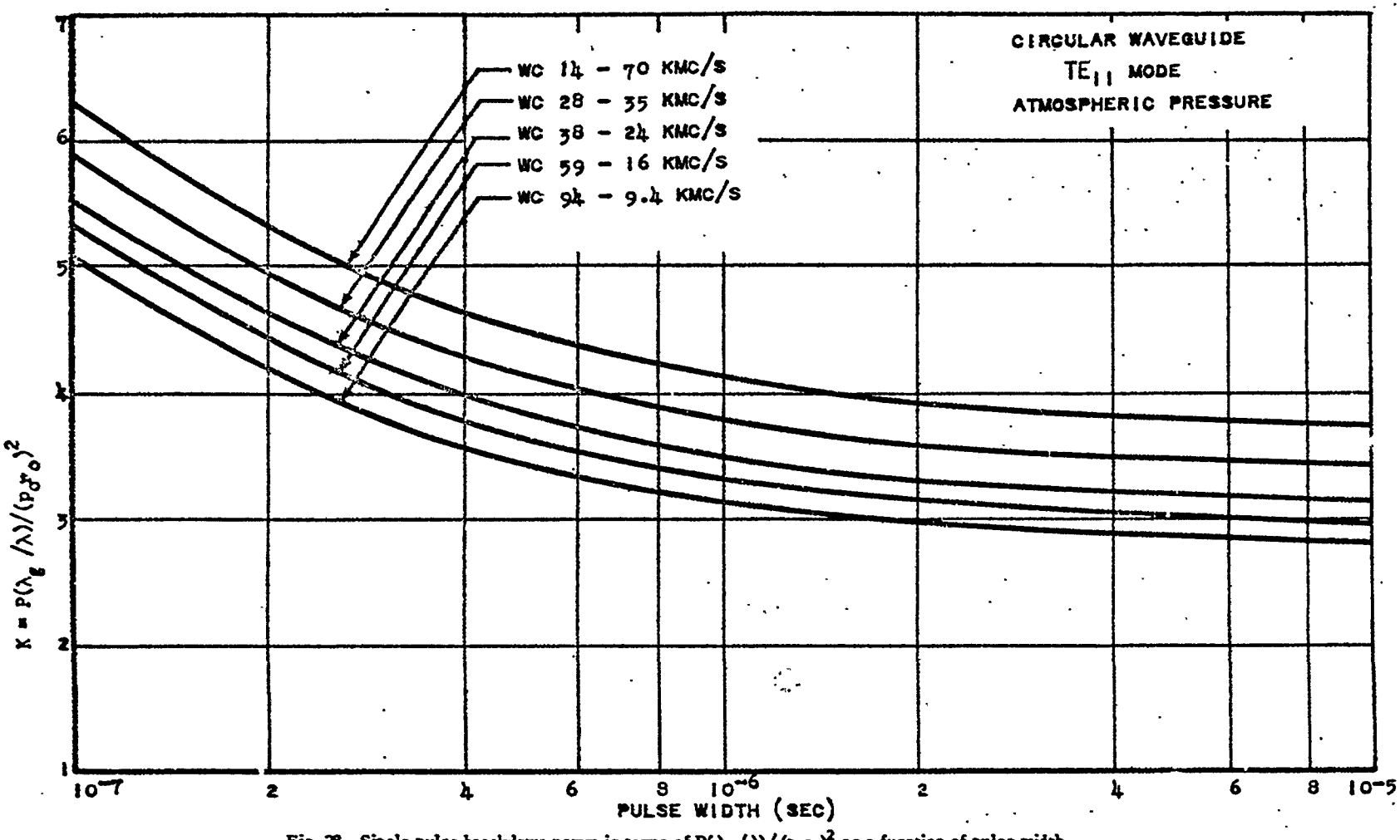

Fig. 28 Single pulse breakdown power in terms of $P(\lambda_g/\lambda)/(p_o r_o)^2$ as a function of pulse width at atmospheric pressure for circular waveguide operating in the TE_{11} mode.

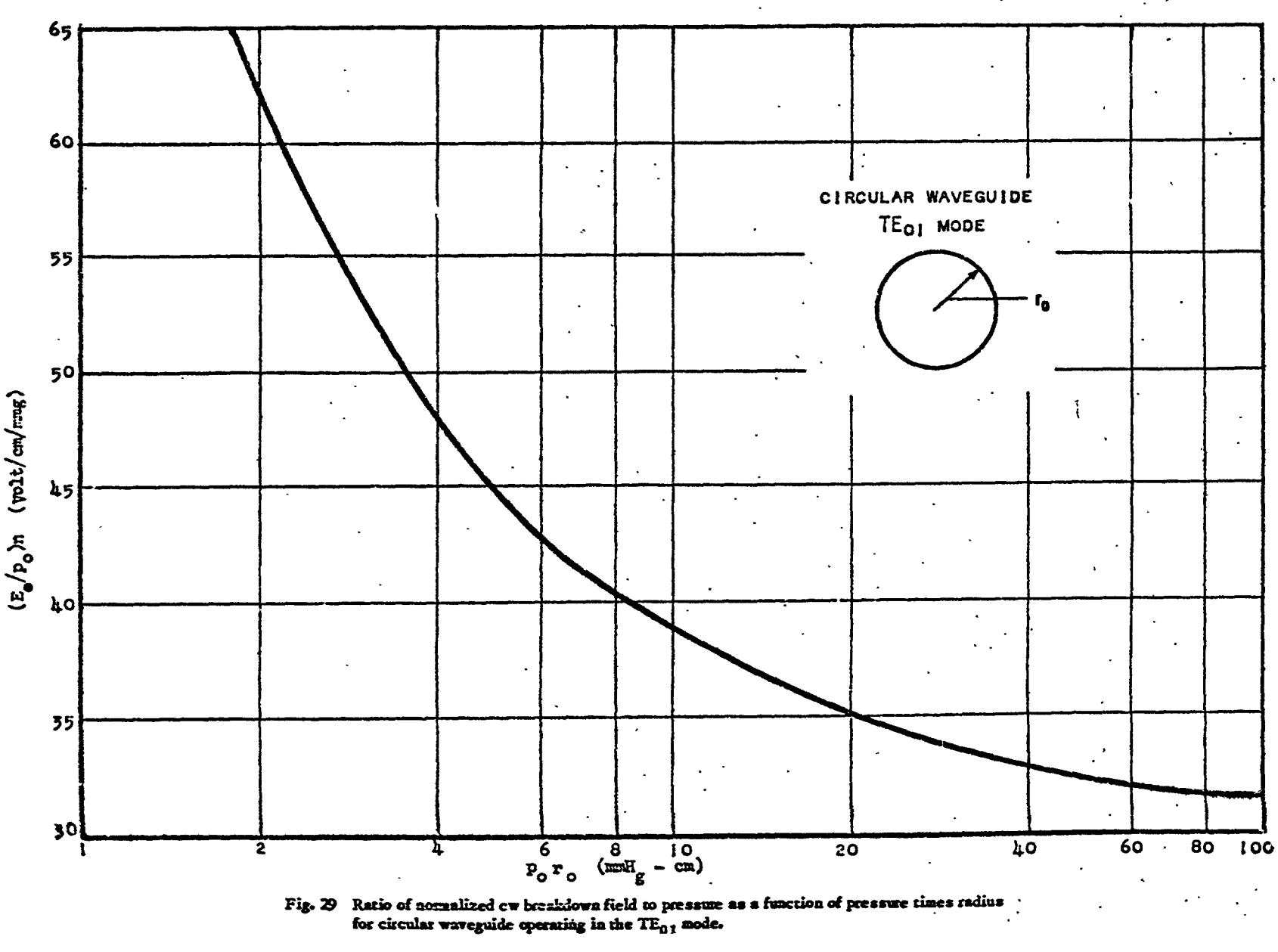

Fig. 29 Ratio of normalized cw breakdown field to pressure as a function of pressure times radius for circular waveguide operating in the TE_{01} mode.

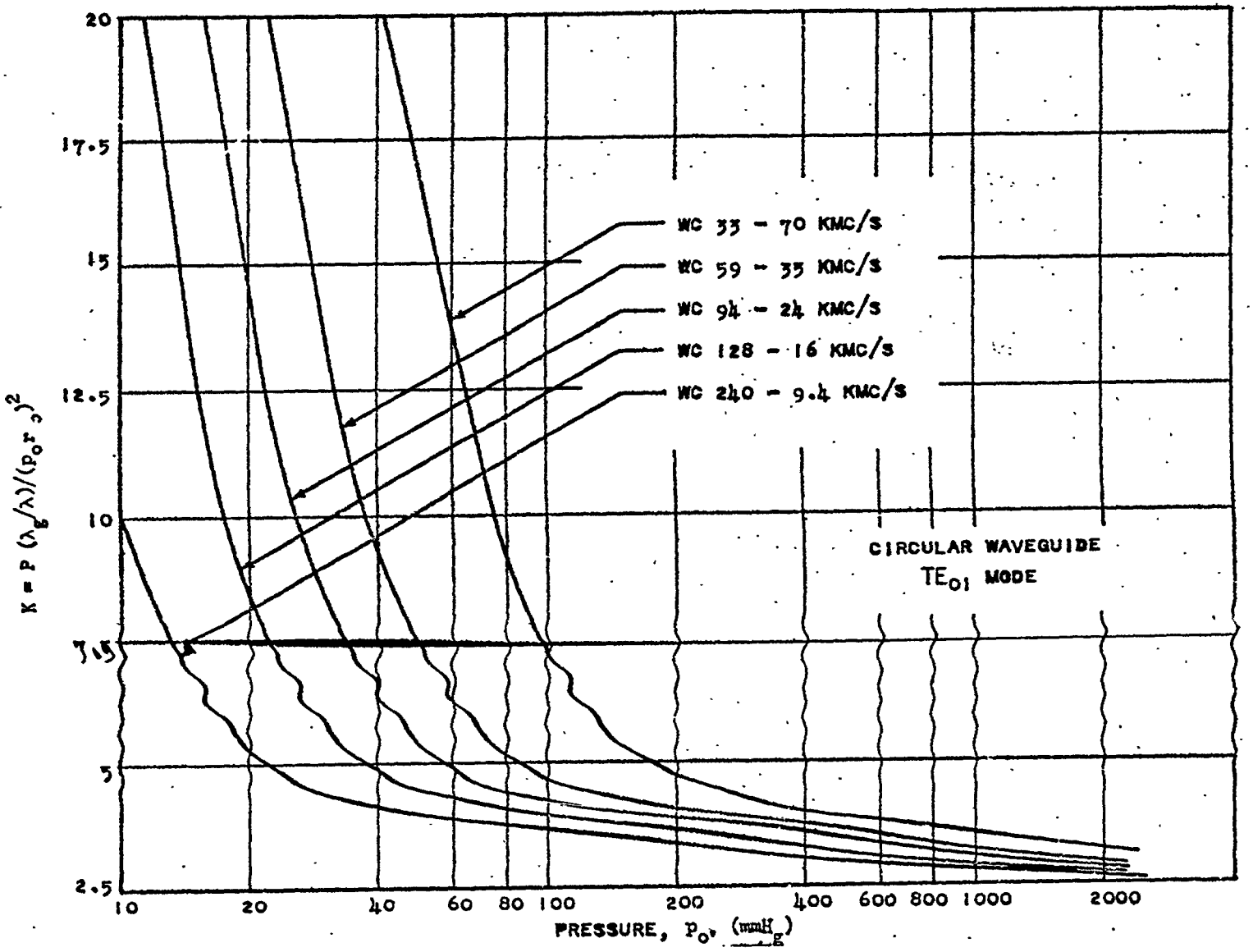

Fig. 30 CW breakdown power in terms of $P(\lambda_g/\lambda)/(p_0 r_0)^2$ as a function of pressure for circular waveguide operating in the TE_{01} mode.

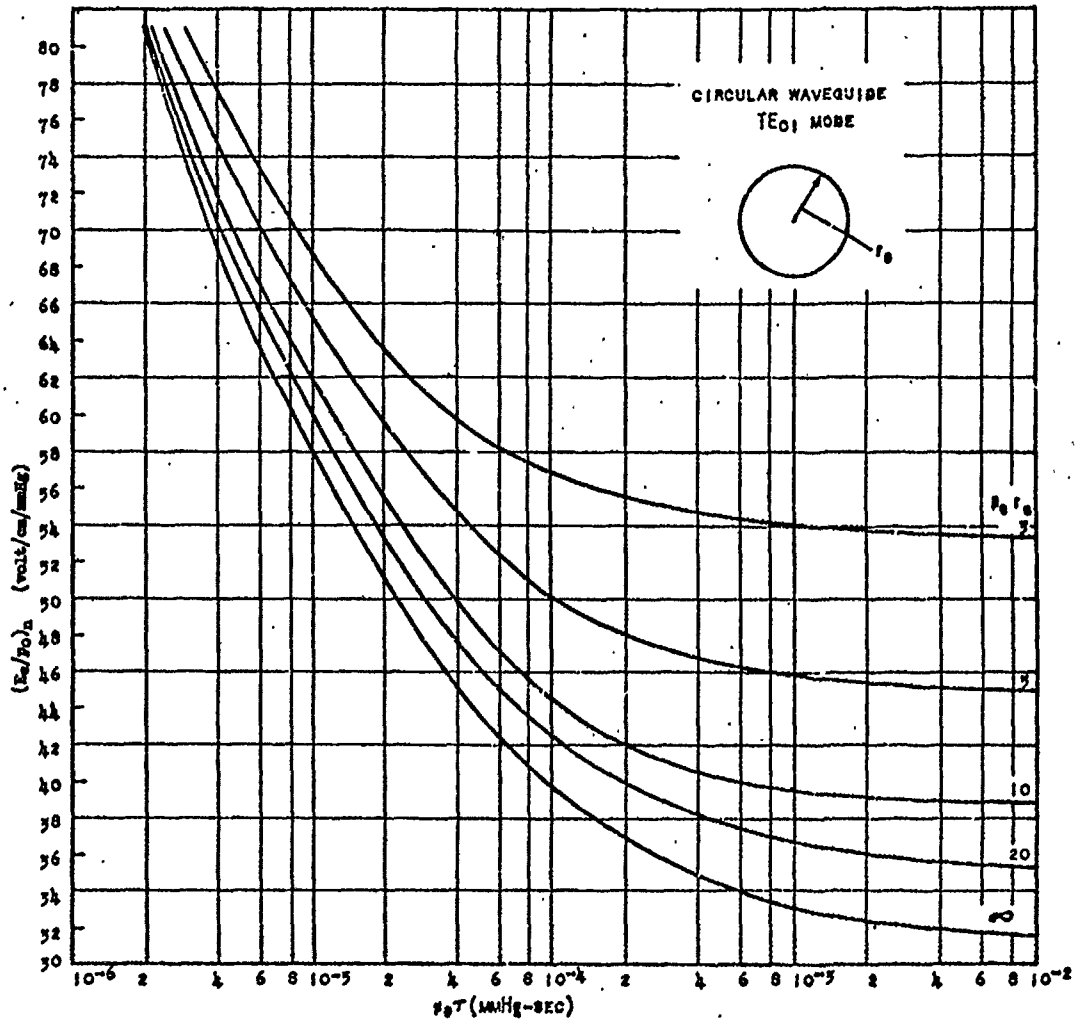

Fig. 31 Ratio of normalized single pulse breakdown field to pressure as a function of pressure times pulse width for various values of pressure times radius for circular waveguides operating in the TE_{01} mode.

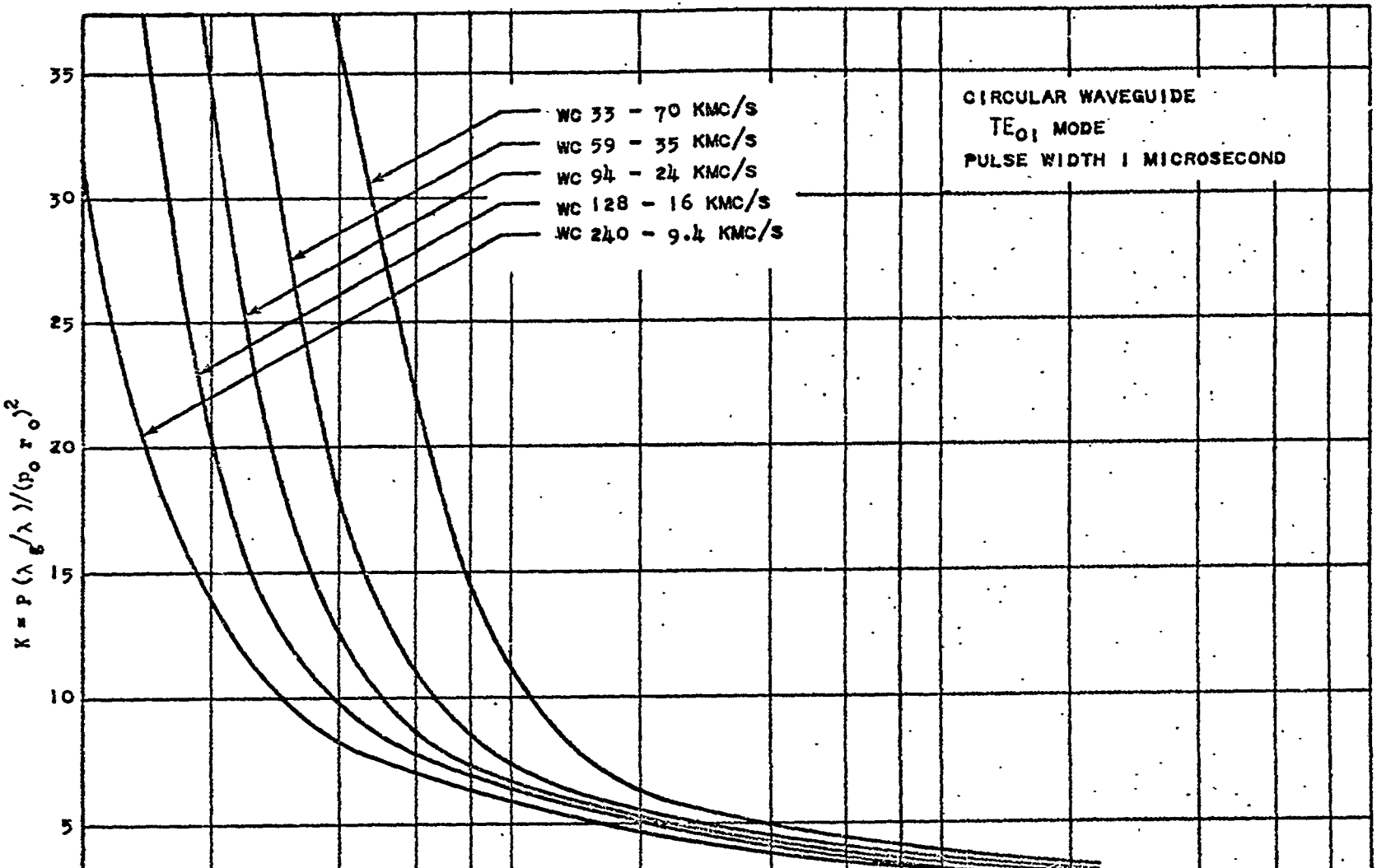

Fig. 32 Single pulse breakdown power in terms of $P(\lambda_g/\lambda)/(p_0 r_0)^2$ as a function of pressure for

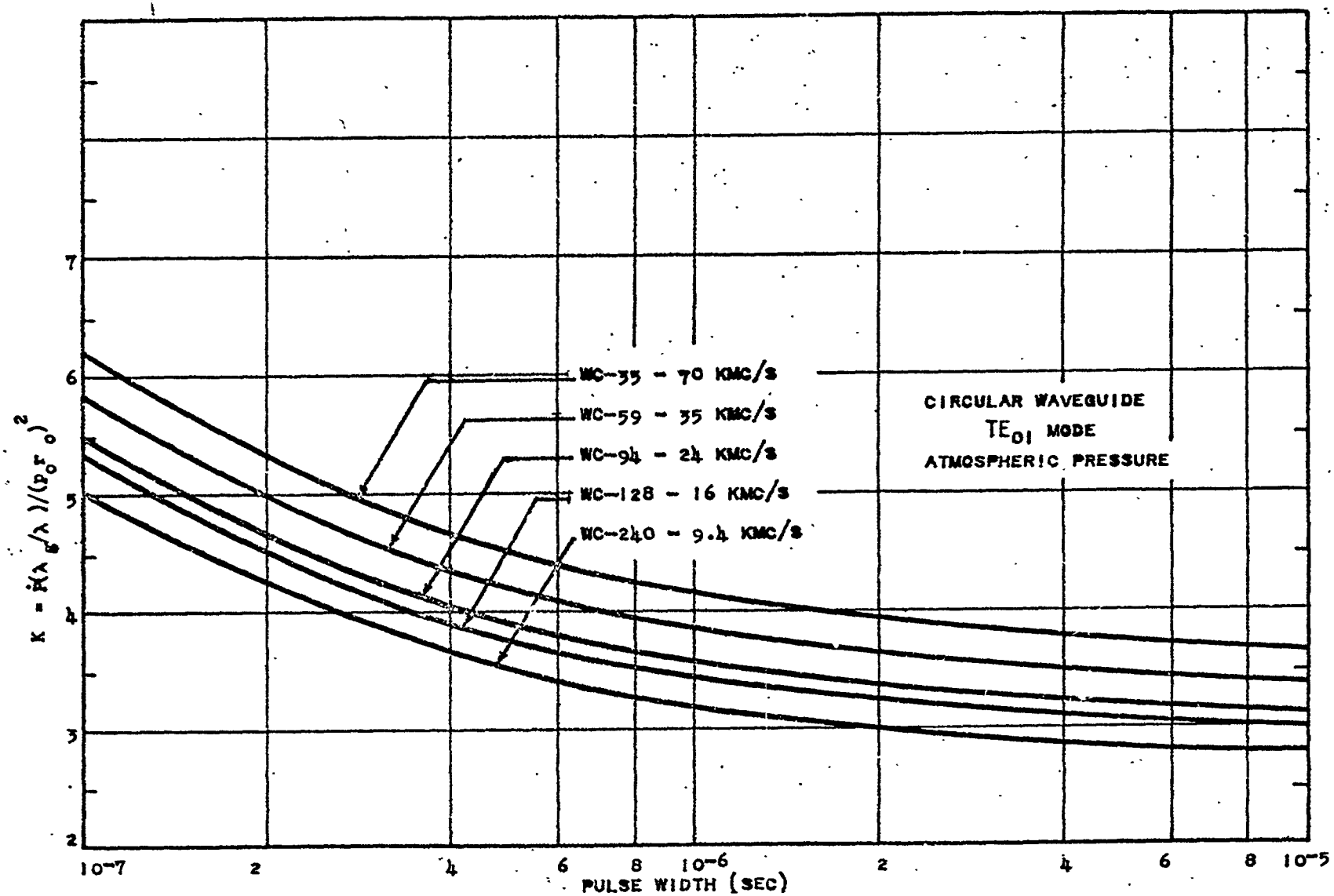

Fig. 33 Single pulse breakdown power in terms of $P(\lambda_g/\lambda)/(p_o r_o)^2$ as a function of pulse width at atmospheric pressure for circular waveguide operating in the TE_{01} mode.

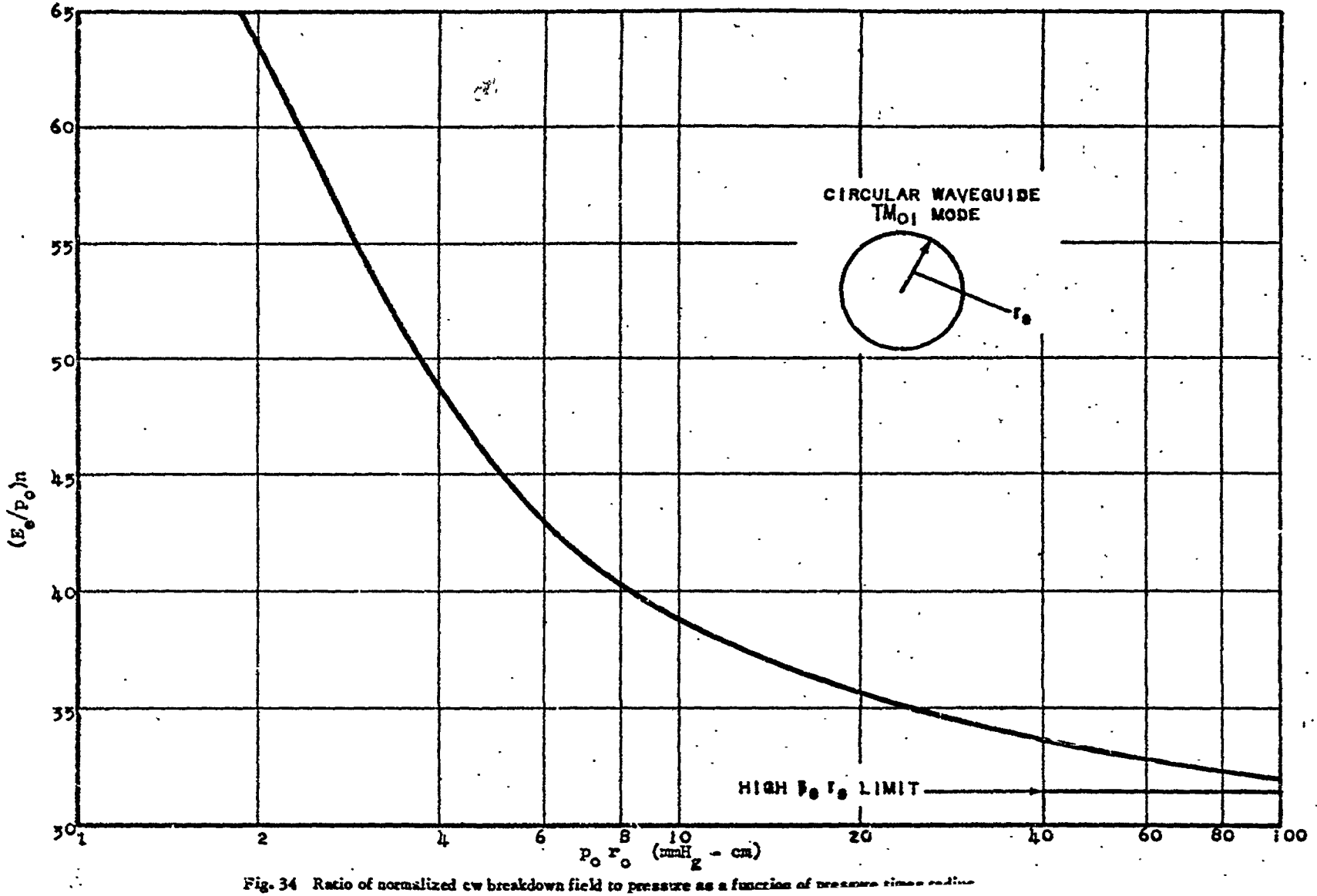

Fig. 34 Ratio of normalized cw breakdown field to pressure as a function of pressure times radius

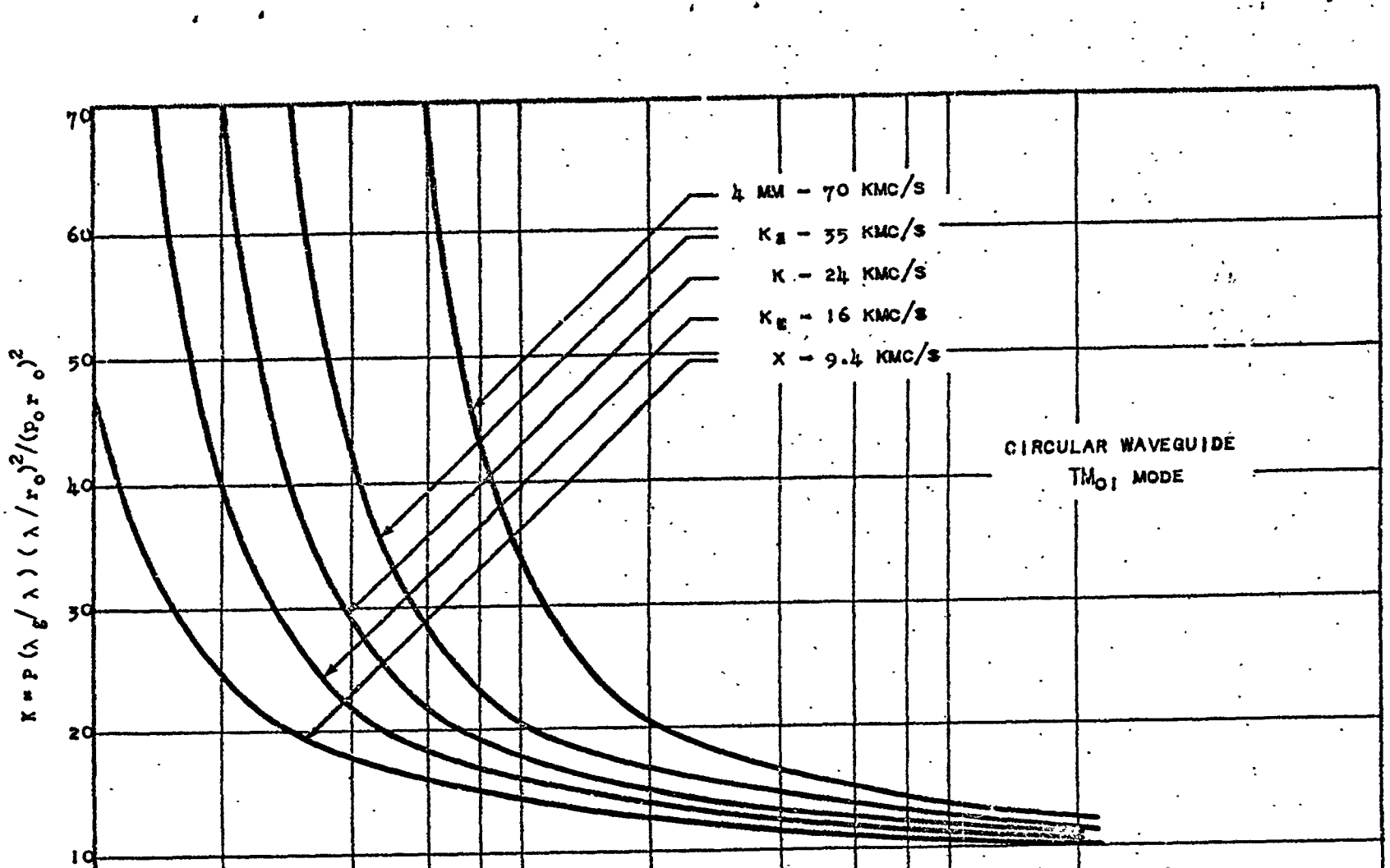
4 MM – 70 KMC/S
K_a – 35 KMC/S
K – 24 KMC/S
K_e – 16 KMC/S
X – 9.4 KMC/S
CIRCULAR WAVEGUIDE
TM_{01} MODE
$K = P(\lambda_g/\lambda)(\lambda/r_0)^2/(p_0 r_0)^2$
PRESSURE, p_0 (mmHg)
0
10
20
30
40
50
60
70
10
20
40
60
80
100
200
400
600
800
1000
2000

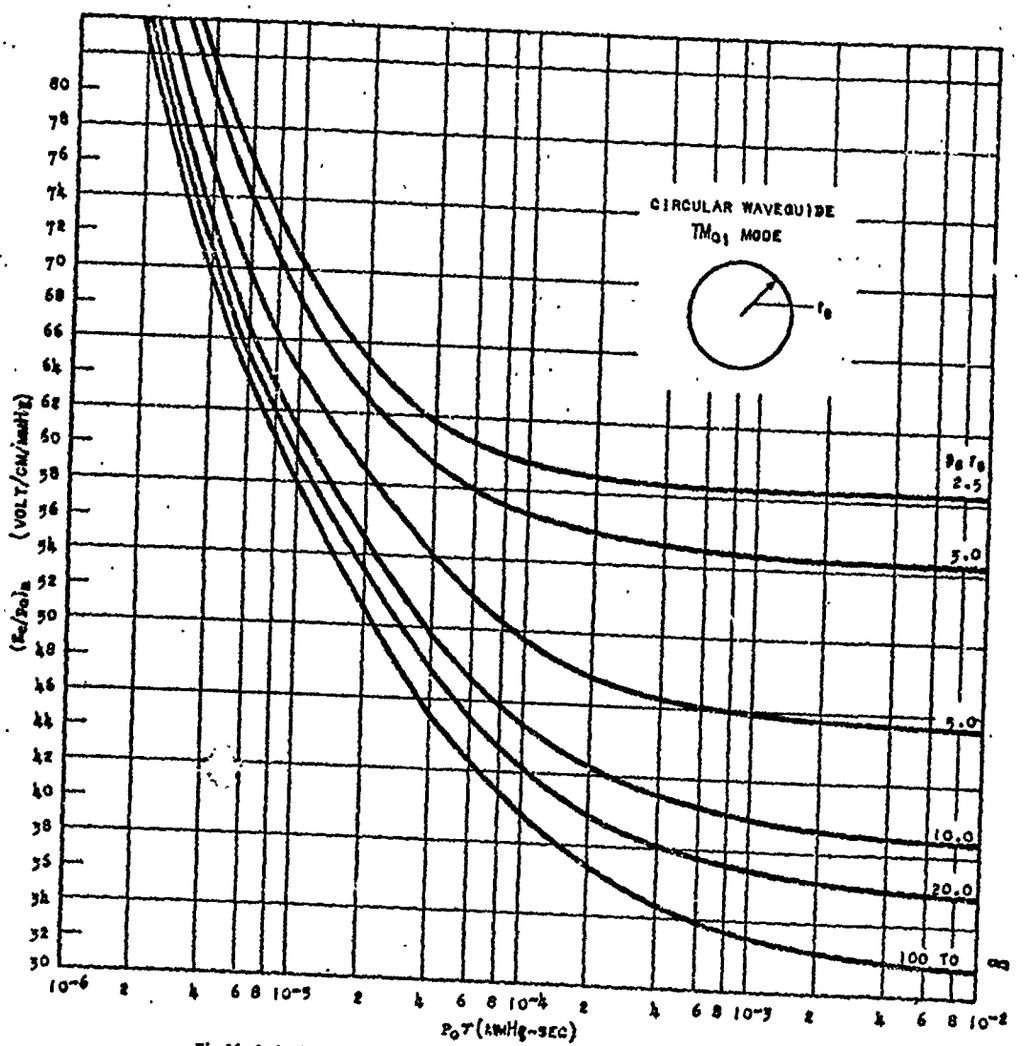

Fig. 36 *Ratio of normalized single pulse breakdown field to pressure as a function of pressure times pulse width for various values of pressure times radius for circular waveguides operating in the* TM_{01} *mode.*

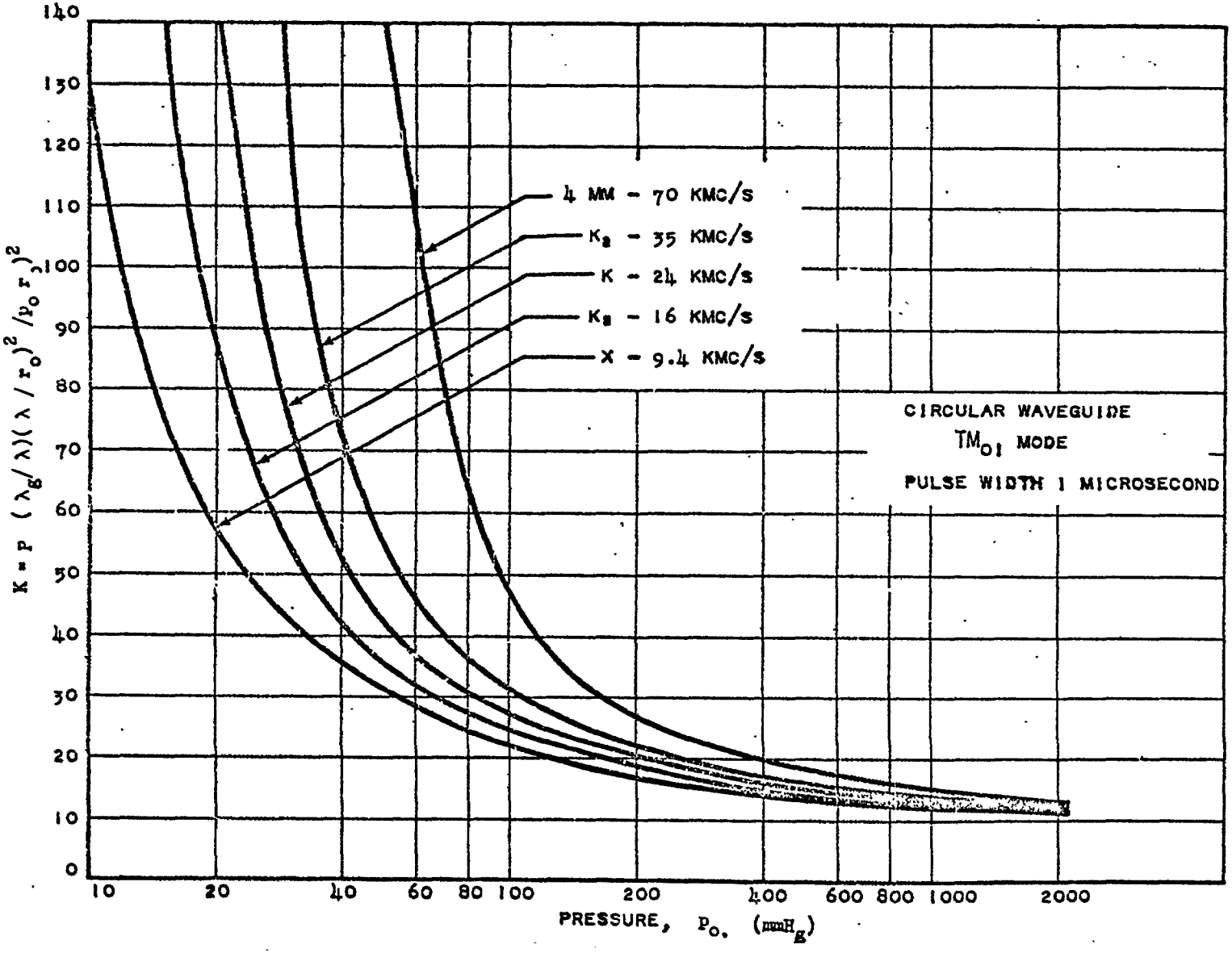
140
130
120
110
100
90
80
70
60
50
40
30
20
10
0
$K = P\ (\lambda_g/\lambda)(\lambda/r_o)^2/p_o r_o)^2$
4 MM - 70 KMC/S
K_a - 35 KMC/S
K - 24 KMC/S
K_g - 16 KMC/S
X - 9.4 KMC/S
CIRCULAR WAVEGUIDE
TM_{01} MODE
PULSE WIDTH 1 MICROSECOND
10
20
40
60
80
100
200
400
600
800
1000
2000
PRESSURE, P_o, (mmH_g)

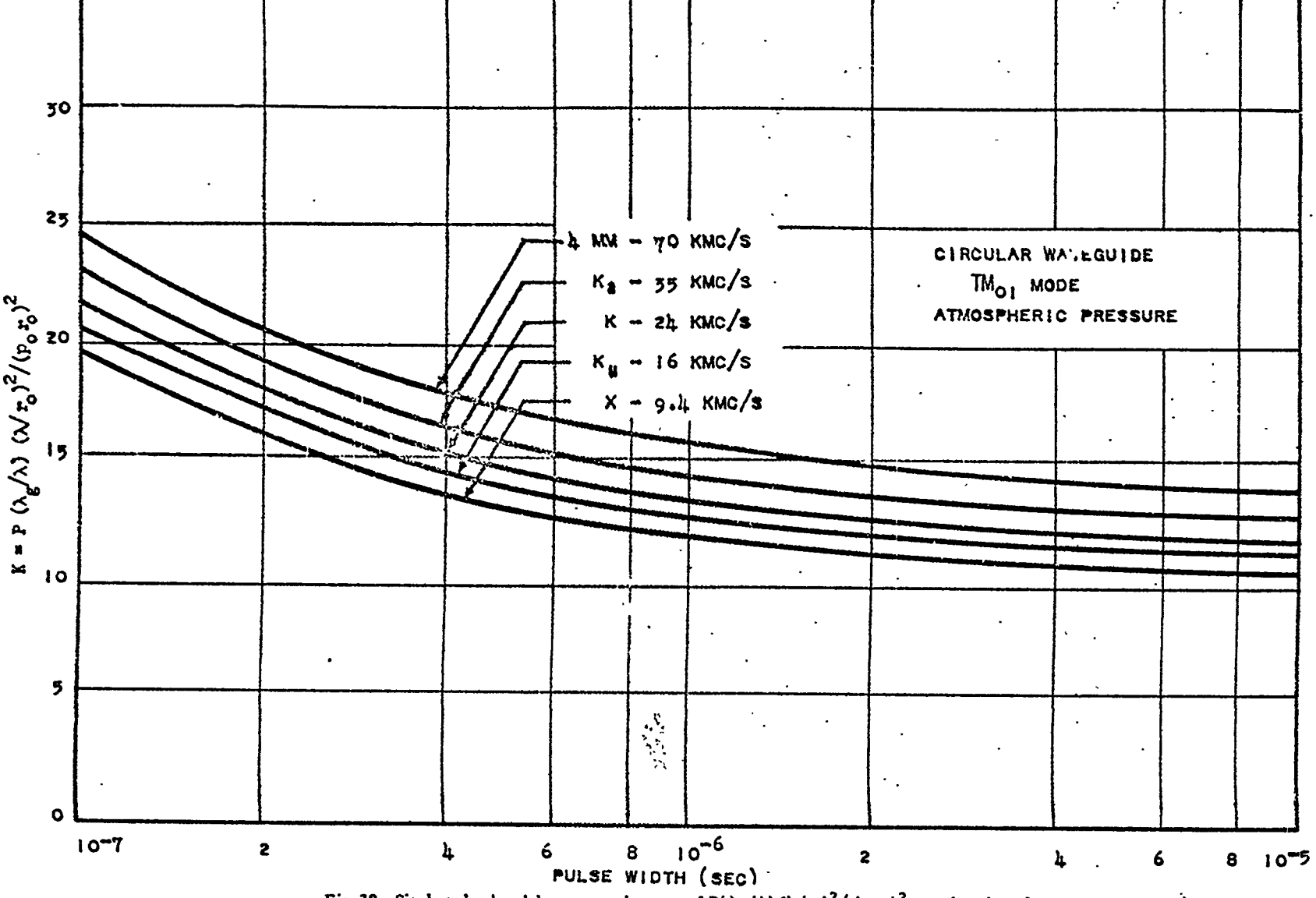

Fig. 38 Single pulse breakdown power in terms of $P(\lambda_g/\lambda)(\lambda/r_0)^2/(p_0 r_0)^2$ as a function of